D-A058 330 COLORADO STATE UNIV FORT COLLINS DEPT OF ELECTRICAL --ETC F/G 20/9
INVESTIGATIONS OF THE DYNAMICS OF MHD FLOWS.(U)
JAN 78 N00014-76-C-0985

NCLASSIFIED

1 OF

AD A058 330

END
DATE FILMED
10-78
DDC

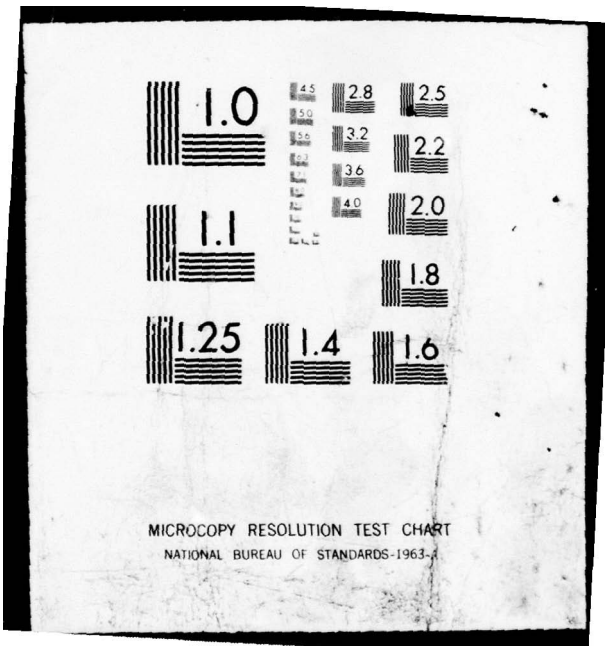
1.0
1.1
1.25
1.4
1.6
1.8
2.0
2.2
2.5
2.8
3.2
3.6
4.0
4.5
5.0
5.6
MICROCOPY RESOLUTION TEST CHART
NATIONAL BUREAU OF STANDARDS-1963-A

AD No. ADA058330
DDC FILE COPY

(1) 5c

OFFICE OF NAVAL RESEARCH
(15) Contract N00014-76-C-0985

LEVEL II

(9) FINAL TECHNICAL REPORT.

(6) INVESTIGATIONS ON THE DYNAMICS OF MHD FLOWS .

Approved for public release; distribution unlimited.
Reproduction in whole or in part is permitted for any purpose of the United States government, and a statement indicating that the research was sponsored by the Office of Naval Research and include the contract and Work Unit numbers.

DDC
RECEIVED
AUG 31 1978
A

Department of Electrical Engineering
Colorado State University
Fort Collins, Colorado

(11) 10 January 1978 (12) 53p.

Reproduction in whole or in part is permitted for any purpose of the United States Government. Qualified requestors may obtain copies of this report from DDC.

H06 434
78 06 26 077
78 08 30 036

Department of Electrical Engineering

Colorado State University
Fort Collins, Colorado
80523

January 20, 1978

Dr. J. A. Satkowski, Director
Power Program, Code 473
Office of Naval Research
800 North Quincy Street
Arlington, VA 22217

Ref: Final Technical Report, "Investigations on the Dynamics of MHD Flows," ONR-Contract N00014-76-C-0985.

Dear Sir:

On 10 January 1978, I mailed to various offices of the Office of Naval Research, the above final report, under the false contract number: N00014-75-C-0213. Please have this number changed to N00014-76-C-0985 on the cover page, page number 1, and the DD Form 1473. Copies of the corrected pages are attached for your convenience.

The erroneous contract number was brought to my attention by courtesy of Mr. R. P. Thacker, ONR representative, Denver.

Please accept my apologies for this oversight.

Sincerely yours,

H. E. Wilhelm
Professor
Electrical Engineering

HEW:fr

attachment

cc: Mr. R. P. Thacker
Dr. E. Florence
Mr. M. A. Chaszeyka
Recipients of Report as specified in distribution list

Security Classification

DOCUMENT CONTROL DATA - R & D

(Security classification of title, body of abstract and indexing annotation must be entered when the overall report is classified)

1. ORIGINATING ACTIVITY (Corporate author) Colorado State University Department of Electrical Engineering Fort Collins, Colorado 80523	2a. REPORT SECURITY CLASSIFICATION Unclassified 2b. GROUP None

3. REPORT TITLE

Investigations on the Dynamics of MHD Flows.

4. DESCRIPTIVE NOTES (Type of report and inclusive dates)

Final Technical Report

5. AUTHOR(S) (First name, middle initial, last name)

H. E. Wilhelm

6. REPORT DATE	7a. TOTAL NO. OF PAGES	7b. NO. OF REFS
10 January 1978	48	49

8a. CONTRACT OR GRANT NO.	9a. ORIGINATOR'S REPORT NUMBER(S)
N00014-~~75~~-76-C-0985 new b. PROJECT NO.	None
c.	9b. OTHER REPORT NO(S) (Any other numbers that may be assigned this report)
d.	None

10. DISTRIBUTION STATEMENT

Reproduction in whole or in part is permitted for any purpose of the United State Government. Qualified requestors may obtain copies of this report from DDC.

11. SUPPLEMENTARY NOTES	12. SPONSORING MILITARY ACTIVITY
None	Power Program Office of Naval Research Arlington, VA

13. ABSTRACT

Exact similarity solutions are derived for the incompressible flow of electrically conducting, viscous fluids across i) homogeneous, axial magnetic fields and ii) nonuniform, azimuthal magnetic fields in diffusers with plane walls. The velocity distributions in the MHD diffusers, the onset of flow separation, and the control of separation by means of magnetic fields are discussed under consideration of induced magnetic fields and viscous stress relaxation. The Stark-effect and (absorbtion) satellite spectra in Helium plasma flows with homogeneous magnetic fields are calculated in presence of laser radiation. - The report summarizes the research conducted during the final year of ONR-Contract N00014-75-C-0213.

DD FORM 1 NOV 68 1473

Unclassified
Security Classification

C O N T E N T S*)

ACCESSION for
NTIS White Section
DDC Buff Section
UNANNOUNCED
JUSTIFICATION
BY
DISTRIBUTION/AVAILABILITY CODES
Dist. AVAIL. and/or SPECIAL
A

*) The page numbers refer to those at the bottom of the pages of this report.

78 06 26 077
78 08 30 037

INTRODUCTION

This is the final report for ONR-Contract N00014-~~75~~-C-~~0210~~ 76 0985, "Investigations on the Dynamics of MHD Flows." The contract has been concerned with MHD flows in diffusers and liquid-metal brushes, and, to a minor extent, with the spectroscopy of Helium plasma flows in homogeneous magnetic fields.

In Chapter II, an exact similarity solution is presented for MHD flows in plane diffusers when the external magnetic field $\vec{B}_o$ is homogeneous and parallel to the apse line of the diffuser walls. For this geometry, the induced magnetic field is in the axial direction, too, so that the Lorentz force is irrotational, $\nabla \times (\vec{j} \times \vec{B}) = \vec{0}$. It is shown that the magnetic field changes the pressure distribution in the flow, but does not directly affect the velocity field of the flow and the onset of flow separation. MHD diffusers with axial, homogeneous magnetic fields are, therefore, not of advantage for MHD generators since they do not permit to control flow separation by means of the applied magnetic field.

In Chapter III, a similarity theory for MHD diffuser flows with viscous stress relaxation is presented when the external magnetic field is azimuthal, $\vec{B}_o(r) \propto r^{-1}\vec{e}_\theta$ (induced magnetic fields are neglected assuming small magnetic Reynolds numbers, $R_M << 1$), together with a kinetic discussion of viscous stress relaxation. We show that viscous stress relaxation changes the form of the velocity field at low Reynolds numbers R and reduces the critical duct angle θ_o^s for flow separation for Hartmann numbers $H^2 \leq 2R/3$, and that flow separation is inhibited for $H^2 > 2R/3$ at any duct angle $\theta_o < \pi$.

In Chapter IV, an exact similarity solution for MHD diffuser flows (without viscous stress relaxation) in an azimuthal magnetic field

$\vec{B}_o(r) \propto r^{-1}\vec{e}_\theta$ is presented, under consideration of the induced magnetic field which is radial. Since the magnetic Reynolds number of MHD flows is generally not large, $R_M \lesssim 1$, we could demonstrate quantitatively that the effect of the induced magnetic fields on the velocity distribution and the onset of separation is small. This result justifies the neglection of induced magnetic fields in various previous investigations on MHD flows.

In Chapter V, the Stark-effect in Helium plasmas with homogeneous magnetic fields is evaluated for absorbtion spectroscopy in presence of laser radiation of advanced generator flows. It is shown that the laser radiation changes qualitatively and quantitatively the satellite spectra, and that the investigations on this subject in the literature are insufficient.

Considerable analytical and numerical effort was expanded in studying the influence of the Hall-effect on MHD diffuser flows. Unfortunately, this investigation could not be completed in time for this final report. An account of the latter work will be communicated as soon as the doctoral research of S. H. Choi has been completed.

NONLINEAR BOUNDARY-VALUE PROBLEM FOR SELFSIMILAR MAGNETOHYDRODYNAMIC DIFFUSER FLOWS ACROSS HOMOGENEOUS MAGNETIC FIELDS*

By

H. E. Wilhelm and S. H. Choi

Abstract

Similarity transformations and selfsimilar solutions are derived for the incompressible radial flow of conducting, viscous fluids across an external, homogeneous magnetic field (parallel to the apse-line) in a diffuser with electrodes in the planes $\theta = \pm\theta_o$ (cylindrical coordinate system). The conducting flow across the (axial) external and induced magnetic fields induces radial and azimuthal current densities, of which only the azimuthal current density produces a net current flux $I \neq 0$ through the electrodes, presumed that these are connected by an external circuit. The eigenvalue problems for the radial velocity and induced magnetic field amplitudes $f(\theta)$ and $\psi(\theta)$ are solved in closed form. The external and induced magnetic fields are shown to change significantly the pressure distribution in the flow, but do not directly influence the velocity distribution and the onset of flow separation. This is due to the irrotational nature of the Lorentz force, $\nabla \times [\nabla \times \vec{B} \times \vec{B}] = \vec{0}$, due to the axial (non-curved) magnetic field $\vec{B}(r,\theta)$.

*) Supported by the U.S. Office of Naval Research

INTRODUCTION

Analytical similarity solutions for electrically conducting, incompressible flows between inclined plane walls ("diffuser") exist in presence of azimuthal external magnetic fields if induced magnetic fields are neglected[1] or considered[2] (depending on the magnitude of the magnetic Reynolds number), and even if viscous stress relaxation is taken into account[3]. For compressible plasma flows in diffusers with azimuthal magnetic fields, closed-form solutions were obtained in the polytropic approximation[4], whereas the general case with heat transfer and Ohmic and viscous heating required both similarity and numerical methods[5,6]. If the applied magnetic field $\vec{b}_o$ is azimuthal, the force field $\vec{j} \times \vec{b}$ resulting from the interaction of the current density $\vec{j}$ and magnetic induction $\vec{b}$ is rotational, $\nabla \times (\vec{j} \times \vec{b}) = \mu_o^{-1} \nabla \times (\vec{b} \cdot \nabla \vec{b}) \neq \vec{0}$, since $\vec{b} \cdot \nabla \vec{b} \neq \vec{0}$ (curved $\vec{b}$-lines). As a consequence, the velocity field $\vec{v}$ in the diffuser is modified by the Lorentz force, whereas the pressure distribution is similar to that of the (nonconducting) Hamel flow[7]. Similarity solutions for magnetohydrodynamic flows in diffusers with homogeneous external magnetic fields have not been found previously. We will demonstrate that a two-dimensional (r,θ) similarity solution exists also for incompressible magnetohydrodynamic diffuser flows, if the applied magnetic field is homogeneous and in the axial direction (z). The induced magnetic field is then also axial (and z-independent) so that the magnetic force density is irrotational, $\nabla \times (\vec{j} \times \vec{b}) = \vec{0}$, since $\vec{j} \times \vec{b} = -\nabla(\vec{b}^2/2\mu_o) + \mu_o^{-1} \vec{b} \cdot \nabla \vec{b}$ where $\vec{b} \cdot \nabla \vec{b} = \vec{0}$ (straight b-lines). In the latter case, therefore, the magnetic volume force changes the pressure distribution in the flow but does not affect the velocity field directly.

We present a similarity transformation which transforms the magnetohydrodynamic equation of motion for the velocity field $\vec{v}(r,\theta)$ and the induction equation for the magnetic field $\vec{b}(r,\theta)$ for the incompressible diffuser flow with an applied homogeneous field $\vec{b}_o$ in the axial direction into nonlinear coupled differential equations for the amplitude fields $f(\theta)$ and $\psi(\theta)$ of $\vec{v}(r,\theta)$ and $\vec{b}(r,\theta)$, respectively. The boundary-value problem for $f(\theta)$ is solved in closed form, whereas the eigen-value problem for $\psi(\theta)$ is treated by means of perturbation theory assuming magnetic Reynolds numbers $R_M \lesssim 1$ ($R_M > 1$ is generally not encountered in experiments)[8]. Graphs of the velocity and magnetic field are presented. The pressure distribution and the onset of separation of the laminar boundary layer from the walls in the magnetohydrodynamic flow are discussed.

BOUNDARY-VALUE PROBLEM

We consider the radial outflow $\vec{v} = \{u,0,0\}$ of a viscous, electrically conducting incompressible fluid (liquids such as mercury or subsonic, quasi-incompressible plasmas) in a diffuser with plane walls at $\theta = \pm\theta_o$ and a homogeneous magnetic field $\vec{b}_o = \{0, 0, b_o\}$ in the axial direction (Fig. 1). The diffuser walls extend radially from $r_1 > 0$ to $r_2 < \infty$ and are ideal conductors which collect the aximuthal currents j_θ which are induced by the radial flow of the conducting fluid across the magnetic field $\vec{b}_o$ in the z-direction. The electrodes are connected by a load circuit through which the current i (amp) is transported. Boundary effects at the remaining insulating walls in the planes $z = \pm z_\infty$ are not considered by assuming that $2z_\infty >> \theta_o(r_1+r_2)/2$, so that all flow fields are two-dimensional of the form $F = F(r,\theta)$. Similarly, hydrodynamic and electromagnetic entrance ($r=r_1$) and exit ($r=r_2$) effects are disregarded. In

actual diffuser flows, end-effects are minimized by operating the diffuser in a similar, larger diffuser duct through which the working fluid is pumped.

For fields independent of z, Maxwell's equation $\nabla \times \vec{b} = \mu_o \vec{j}$ indicates that the azimuthal current density $j_\theta(r,\theta)$ produces an axial magnetic field $b_z(r,\theta)$, which in turn requires a radial current density $j_r(r,\theta)$ since

$$\mu_o j_\theta = -\partial b_z/\partial r, \quad \mu_o j_r = +r^{-1}\, \partial b_z/\partial \theta.$$

It is also seen that the fields $\vec{j} = \{j_r, j_\theta, 0\}$ and $\vec{b} = \{0,0,b_o + b_z\}$ satisfy the basic equations $\nabla\cdot\vec{j} = 0$ and $\nabla\cdot\vec{b} = 0$. In accordance with the current transport equation, $\vec{j} = \sigma(\vec{e} + \vec{v} \times \vec{b})$ in absence of the Hall-effect[8], the electric field is of the form $\vec{e} = \{e_r, e_\theta, 0\}$ and satisfies the basic equation $\nabla \times \vec{e} = \vec{0}$. We introduce dimensionless flow fields and independent variables in accordance with (p = pressure field),

$$U(\rho,\theta) = u(r,\theta)/u_o, \; P(\rho,\theta) = p(r,\theta)/p_o, \; J_{\rho,\theta}(\rho,\theta) = j_{r,\theta}(r,\theta)/j_o, \tag{1}$$

$$B(\rho,\theta) = b_z(r,\theta)/b_o, \; B_o = 1, \; E_{\rho,\theta}(\rho,\theta) = e_{r,\theta}(r,\theta)/e_o, \tag{2}$$

and

$$\rho = r/r_o, \quad r_o \in (r_1,r_2) \tag{3}$$

where

$$u_o = u(r_o,0) > 0, \; p_o = \rho_o u_o^2, \; e_o = u_o b_o, \; j_o = \sigma u_o b_o \tag{4}$$

Based on the magnetohydrodynamic equations for constant density ρ_o, viscosity μ, and conductivity σ and Maxwell's equations, we derive for the dimensionless fields $U(\rho,\theta)$, $P(\rho,\theta)$, and $B(\rho,\theta)$ of the plane diffuser with axial external magnetic field the nonlinear boundary-value problem:

$$U\frac{\partial U}{\partial \rho} = -\frac{\partial}{\partial \rho}\left[P + \frac{1}{2}N(1+B)^2\right] + \frac{R^{-1}}{\rho^2}\frac{\partial^2 U}{\partial \theta^2} \quad , \quad (5)$$

$$0 = \frac{\partial}{\partial \theta}\left[-P - \frac{1}{2}N(1+B)^2 + 2R^{-1}\frac{U}{\rho}\right] \quad , \quad (6)$$

$$\frac{\partial U}{\partial \rho} + \frac{U}{\rho} = 0 \quad , \quad (7)$$

$$\frac{\partial^2 B}{\partial \rho^2} + \frac{1}{\rho}\frac{\partial B}{\partial \rho} + \frac{1}{\rho^2}\frac{\partial^2 B}{\partial \theta^2} = R_M \frac{1}{\rho}\frac{\partial}{\partial \rho}\left[\rho U(1+B)\right] \quad , \quad (8)$$

with

$$U(\rho,\theta)_{\theta=\pm\theta_o} = 0, \quad \rho_1 \leq \rho \leq \rho_2 \quad , \quad (9)$$

$$\left[\partial B(\rho,\theta)/\partial\theta\right]_{\theta=\pm\theta_o} = 0, \quad \rho_1 \leq \rho \leq \rho_2 \quad , (10)$$

$$\int_{-\theta_o}^{+\theta_o} U(\rho,\theta)\,\rho d\theta = Q > 0 \quad , (11)$$

$$\int_{\rho_1}^{\rho_2} \left[\partial B(\rho,\theta)/\partial\rho\right]_{\theta=\pm\theta_o} d\rho = -R_M I \quad . (12)$$

$q = \rho_o u_o r_o\, Q$ and $i = j_o r_o I$ are the dimensional flow rate and dimensional load current, each per unit length $\Delta z = 1$. Although asymmetric Hamel flows are compatible with the basic equations and boundary conditions[7], we consider exclusively symmetric outflows with

$$U(\rho,-\theta) = U(\rho,+\theta), \quad B(\rho,-\theta) = B(\rho,+\theta) \quad . \quad (13)$$

The flow Reynolds number R, the magnetic Reynolds number R_M, and the energy ratio N are defined as

$$R = u_o r_o \rho_o/\mu, \quad R_m = \sigma\mu_o u_o r_o, \quad N = (b_o^2/\mu_o)/\rho_o u_o^2 \quad . \quad (14)$$

Eqs. (5-6), (7), and (8) are the equation of motion (r and θ components), the continuity equation, and the induction equation $[\nabla^2\vec{b} = -\mu_o\sigma\,\nabla \times (\vec{v}\times\vec{b})]$, respectively. The boundary conditions (9) and (10) consider that the

fluid does not slip at the walls $\theta = \pm\theta_o$ and that $E_\rho(\rho,\pm\theta_o) = J_\rho(\rho,\pm\theta_o) = R_m^{-1}\rho^{-1}\,\partial B(\rho,\pm\theta_o)/\partial\theta = 0$ at the electrodes of infinite conductivity, respectively. Eqs. (12) and (13) specify the (given) mass (Q) and current (I) flows.

From the solutions $U(\rho,\theta)$ and $B(\rho,\theta)$ of Eqs. (5)-(13), the remaining (dimensionless) flow fields are obtained as

$$J_\rho = R_M^{-1}\,\rho^{-1}\,\partial B/\partial\theta, \quad J_\theta = -R_m^{-1}\,\partial B/\partial\rho \qquad ,(15)$$

$$E_\rho = R_M^{-1}\,\rho^{-1}\,\partial B/\partial\theta, \quad E_\theta = U(1+B) - R_M^{-1}\,\partial B/\partial\rho \qquad .(16)$$

SIMILARITY TRANSFORMATION AND EIGENVALUE PROBLEMS

The boundary-value problem in Eqs. (5)-(12) has selfsimilar solutions of the form $F(\rho,\theta) = \rho^\nu\, G(\theta)$ for the velocity field $U(\rho,\theta)$ and the magnetic field $B(\rho,\theta)$, whereas the pressure field $P(\rho,\theta)$ has a more complicated structure. Integration of Eq. (6) yields for the sum of hydrostatic and magnetic pressures

$$P + \frac{1}{2}N(1+B)^2 = 2R^{-1}\frac{U}{\rho} + \beta(\rho) \qquad (17)$$

where $\beta(\rho)$ is an integration "constant" with respect to θ. Elimination of $P + \frac{1}{2}N(1+B)^2$ from Eq. (5) by means of Eq. (17) results in

$$U\frac{\partial U}{\partial\rho} = R^{-1}\left[2\frac{U}{\rho^2} - \frac{2}{\rho}\frac{\partial U}{\partial\rho} + \frac{1}{\rho^2}\frac{\partial^2 U}{\partial\theta^2}\right] - \frac{d\beta(\rho)}{d\rho} \qquad .(18)$$

Alternatively, $\nabla[P + \frac{1}{2}N(1+B)^2]$ could have been eliminated from Eqs. (5)-(6) by taking the curl of the equation of motion. Since $\partial(\rho U)/\partial\rho = 0$ by Eq. (7), Eq. (8) can be reduced to

$$\frac{\partial^2 B}{\partial\rho^2} + \frac{1}{\rho}\frac{\partial B}{\partial\rho} + \frac{1}{\rho^2}\frac{\partial^2 B}{\partial\theta^2} = R_M\, U\frac{\partial B}{\partial\rho} \qquad .(19)$$

It is now seen that Eqs. (18) and (19) can be reduced to ordinary

differential equations by means of the similarity transformation

$$U(\rho,\theta) = f(\theta)/\rho^n, \quad n = 1 \qquad , (20)$$

$$B(\rho,\theta) = \psi(\theta)/\rho^m, \quad m > 0 \qquad , (21)$$

where n = 1 by Eq. (7) and m is a still undetermined eigenvalue, namely:

$$\frac{d^2f}{d\theta^2} + Rf^2 + 4f = R\rho^3 \frac{d\beta(\rho)}{d\rho} \equiv -\alpha R \qquad , (22)$$

$$\frac{d^2\psi}{d\theta^2} + m(m+R_M f)\psi = 0 \qquad . (23)$$

In Eq. (22), αR is a separation constant, and the ρ-dependent constituent of the pressure field becomes

$$\beta(\rho) = \frac{1}{2}\alpha\rho^{-2} + P_\infty \qquad (24)$$

where P_∞ is the hydrostatic overpressure. Combining of Eqs. (17) and (24) gives for the total pressure field

$$P(\rho,\theta) + \frac{1}{2}N[1+B(\rho,\theta)]^2 = 2R^{-1}\frac{f(\theta)}{\rho^2} + \frac{1}{2}\frac{\alpha}{\rho^2} + P_\infty \qquad . (25)$$

Note that the sum of hydrostatic and magnetic pressures is of the same selfsimilar form as the pressure field in the classical Hamel flow[7]. Eqs. (20)-(21) and (25) represent the similarity transformation for the nonlinear magnetohydrodynamic flow problem under consideration.

Eq. (22) and the boundary condition (9) give for the determination of the velocity amplitude $f(\theta)$ the nonlinear eigenvalue problem with eigenvalue α:

$$\frac{d^2f}{d\theta^2} + Rf^2 + 4f + \alpha R = 0 \qquad , (26)$$

$$f(\pm\theta_o) = 0 \qquad , (27)$$

with

$$f(-\theta) = f(+\theta), \quad f(0) \equiv 1 \qquad . (28)$$

Eq. (23) and the boundary conditions (10) and (12) give for the determination of the magnetic field amplitude $\psi(\theta)$ the linear eigenvalue problem with eigenvalue μ:

$$\frac{d^2\psi}{d\theta^2} + \mu\,\psi = -\mu^{\frac{1}{2}} R_M\, f(\theta)\psi\ , \quad \mu \equiv m^2 \qquad , (29)$$

$$d\psi(\pm\theta_o)/d\theta = 0 \qquad , (30)$$

with

$$\psi(-\theta) = \psi(+\theta) \quad \psi(\pm\theta_o) = R_M I(\rho_1^{-\mu^{\frac{1}{2}}} - \rho_2^{-\mu^{\frac{1}{2}}})^{-1} \qquad . (31)$$

In Eq. (4), the identity $f(0) \equiv 1$ is due to the nondimensionalization of $U(\rho,\theta)$ with respect to $u_o = u(r_o,0)$, Eq. (4). Since $B(\rho,\theta)$ is non-dimensionalized with respect to the arbitrary (external) $b_o \gtrless 0$, $|\psi(0)| \neq 1$ in general in accordance with Eq. (31). In the eigenvalue problem (29)-(31), $f(\theta)$ represents a variable coefficient which is assumed to be known from the solution of Eqs. (26)-(28).

Since $\psi(\theta)$ is an even function of θ, by Eq. (31), $d\psi(\theta)/d\theta$ is an odd function of θ. Hence, the flux of the radial current density $J_\rho(\rho,\theta)$ through any surface $\rho_1 \leq \rho = \text{constant} \leq \rho_2$, $|\theta| \leq \theta_o$, vanishes [Eq. (15)],

$$\int_{-\theta_o}^{+\theta_o} J_\rho\, \rho d\theta = R_M^{-1}\, \rho^{-m} \int_{-\theta_o}^{+\theta_o} \frac{d\psi}{d\theta}\ d\theta = 0 \qquad . (32)$$

SOLUTION FOR $f(\theta)$

We seek symmetrical solutions of the boundary-value problem (26)-(28) which represent pure outflows, $0 \leq f(\theta) \leq 1$. Net outflow solutions ($Q > 0$) with backflow regions where $f(\theta) < 0$ are not discussed since they are in all probability not stable (flow separation). A first integration of

Eq. (26) gives

$$(\frac{df}{d\theta})^2 = \frac{2}{3}R[C - f^3 - 6R^{-1}f^2 - 3\alpha f] \tag{33}$$

where $[df(\pm\theta_o)/d\theta]^2 = (2/3)RC \geq 0$ for $R > 0$. Since $df(0)/d\theta = 0$ and $f(0) = 1$,

$$C = 1 + 6R^{-1} + 3\alpha \geq 0 \quad . \tag{34}$$

Backflows occur at the walls $\theta = \pm\theta_o$ if $df/d\theta \gtrless 0$ for $\theta = \pm\theta_o$. Accordingly, the eigenvalues α of pure outflows are larger than a critical value which is negative,

$$\alpha \geq \tilde{\alpha}, \quad \tilde{\alpha} = -\frac{1}{3}(1+6R^{-1}) \quad . \tag{35}$$

In view of Eq. (34), the trinomial in Eq. (33) has the roots

$$f_1 = 1, \quad f_2 = f_+, \quad f_3 = f_- \tag{36}$$

where

$$f_\pm = \frac{1}{2}\{-(1+6R^{-1}) \pm [(1+6R^{-1})^2 - 12\alpha - 4(1+6R^{-1})]^{1/2}\} \tag{37}$$

with

$$\left.\begin{matrix} f_\pm = \text{conjugate complex} \\ f_\pm = \text{real} \end{matrix}\right\} \text{ for: } \quad \alpha \gtrless -\frac{1}{4}(1+6R^{-1})(1-2R^{-1}) \quad . \tag{38}$$

Formal integration of Eq. (34) yields, under consideration of $f(0) = f_1 = 1$,

$$(2R/3)^{1/2}\theta = \pm \int_1^{f(\theta)} [(-1)(f-f_1)(f-f_2)(f-f_3)]^{-1/2} df \quad . \tag{39}$$

In the evaluation of the elliptic integral [9] in Eq. (39) for pure outflows, $0 \leq f(\theta) \leq 1$, two cases have to be distinguished:

CASE I: $f_\pm$ = conjugate complex.

In this case, the eigenvalues α lie in the region defined by Eq. (38). The substitution $f = f_1 - \lambda^2[(1-\cos\phi)/(1+\cos\phi)]$, $0 \leq \phi \leq \pi$, reduces Eq. (39) to $(2R/3)^{1/2}\,\theta = \mp\,\lambda^{-1}\,F(\phi,k)$. The solution $f(\theta)$ is obtained

by inversion of the elliptic integral $F(\phi,k)$ of the first kind as:

$$f(\theta) = 1 - \lambda^2 \frac{1-\mathrm{cn}[(2R/3)^{1/2}\lambda\theta;k]}{1+\mathrm{cn}[2R/3)^{1/2}\lambda\theta;k]} \tag{40}$$

where

$$\lambda^2 = [3(1+\alpha+4R^{-1})]^{1/2} \quad , \tag{41}$$

$$k^2 = \tfrac{1}{2}[1+\tfrac{3}{2}\lambda^{-2}(1+2R^{-1})] \quad . \tag{42}$$

The eigenvalue α is given by the boundary condition (27) as the real root of the transcendental equation,

$$\mathrm{cn}[(2R/3)^{1/2}\lambda\theta_o;k] = (\lambda^2-1)/(\lambda^2+1) \quad . \tag{43}$$

CASE II: $f_\pm$ = real.

In this case, the eigenvalues lie in the interval, $-(1+6R^{-1})/3 \leq \alpha \leq -(1+6R^{-1})(1-2R^{-1})/4$, and $f_1 > f_2 > f_3$ by Eqs. (36)-(37) since $f_\pm \leq 0$. The substitution $f = f_2 + (f_1-f_2)\cos^2\phi$, $0 \leq \phi \leq \pi/2$, reduces Eq. (39) to $(2R/3)^{1/2}\lambda\theta = \mp \lambda^{-1} F(\phi,k)$. Inversion of the elliptic integral yields the solution:

$$f(\theta) = f_2 + (1-f_2)\mathrm{cn}^2[(2R/3)^{1/2}\lambda\theta;k] \tag{44}$$

where

$$\lambda^2 = (1-f_3)/4 \quad , \tag{45}$$

$$k^2 = (1-f_2)/(1-f_3) \quad . \tag{46}$$

The eigenvalue α is determined by the boundary conditions (27) as the real root of the transcendental equation,

$$\mathrm{cn}^2[(2R/3)^{1/2}\lambda\theta_o;k] = -f_2/(1-f_2) \quad . \tag{47}$$

For large Reynolds numbers, $R \gg 1$, as encountered in most experiments, both Eqs. (40)-(43) and Eqs. (44)-(47) indicate that λ, k, and α - and, hence, the solution $f(\theta/\theta_o)$ - depend only on the combination

$I = R^{1/2}\theta_o$. This means that flows with different R and θ_o, but with the same $I = R^{1/2}\theta_o$, have identical velocity distributions $f(\theta/\theta_o)$. This invariance principle is a special case of the one first discovered for compressible magnetohydrodynamic flows[4].

At the transition from pure outflow, $f(\theta) \geq 0$, to backflow $f(\theta) < 0$ in the vicinity of the walls $\theta = \pm\theta_o$, the azimuthal velocity gradient drops to zero at the walls. This transition point is usually defined as the onset of flow separation in incompressible fluids[10]. Applica- of the condition $df(\pm\theta_o)/d\theta = 0$ to the solution in Eq. (44), which is valid for eigenvalues down to the separation value $\tilde{\alpha} = -(1+6R^{-1})/3$, gives for the critical duct angle $\tilde{\theta}_o$ beyond which separation occurs

$$(2R/3)^{1/2}\tilde{\lambda}\tilde{\theta}_o = K(\tilde{k}) \tag{48}$$

where $K(k)$ is the complete elliptic integral of the first kind[9]. Substitution of Eq. (48) into Eq. (47) shows that $f_2 = 0$ so that at the onset of separation

$$f_1 = 1, \quad f_2 = 0, \quad f_3 = -(1+6R^{-1}) \tag{49}$$

and

$$\tilde{\lambda}_s^2 = (1+3R^{-1})/2, \qquad \tilde{k}^2 = (1+3R^{-1})^{-1}/2 \tag{50}$$

Combining of Eqs. (48)-(50) shows that the critical duct angle $\tilde{\theta}_o$ beyond which ($\theta_o > \tilde{\theta}_o$) flow separation sets in decreases with increasing Reynolds number R,

$$\tilde{\theta}_o = [3/(3+R)]^{-\frac{1}{2}} \quad K(\sqrt{R/(6+2R)}) \quad . \tag{51}$$

Since the eigenvalue $\alpha = -(1+6R^{-1})/3$ is negative at the onset of separation, the total wall pressure $P(\rho,\pm\theta_o) + \frac{1}{2}N[1+B(\rho,\pm\theta_o)]^2$ is positive at the onset of separation by Eq. (25) if the overpressure P_∞ is sufficiently positive.

In order to have a stable, unseparated diffuser flow, experiments

are generally operated at sufficiently positive eigenvalues, $\alpha \geq -(1+6R^{-1})/3$. Fig. 2 gives the eigenvalue α for pure outflows versus the invariance parameter $I = \sqrt{R}\ \theta_o$ ($R \gg 1$) based on Eqs. (43) and (47) for the solutions of types I and II, respectively. α decreases monotonically from large positive values (for large I-values) to its minimum value $\alpha = -1/3$ (for $I = 3.18704$) below which backflows occur at the walls.

Fig. 3 shows the azimuthal distribution $f(x)$, $x = \theta/\theta_o$, of the radial flow velocity of pure outflows for eigenvalues $\alpha = -1/3$ to 5.0 ($I = 3.187$ to 0.591) based on Eqs. (40) and (44) for the solutions of types I and II, respectively. It is seen how $f(x)$ changes from the shape of regular outflows for small values of $I = \sqrt{R}\ \theta_o$ to the critical flow with the maximum value $I = \sqrt{R}\ \theta_o = 3.187$ (of a pure outflow), at which the transition to mixed flows occurs. The curves in Fig. 3 imply large Reynolds numbers, $R \gg 1$, for which the invariance principle holds.

Fig. 4 shows the critical duct angle $\tilde{\theta}_o$, beyond which ($\theta_o > \tilde{\theta}_o$) backflows occur, versus the Reynolds number R based on Eq. (51), It is recognized that $\tilde{\theta}_o$ decreases rapidly with increasing R. Pure (unseparated) outflows can, therefore, only be achieved at large Reynolds numbers R if the duct angle is sufficiently small, $\theta_o \leq \tilde{\theta}_o(R)$. It should be noted that in the present case of a homogeneous, axial $\vec{b}_o$, the external magnetic field can not prevent flow separation, in contrast to an azimuthal, external magnetic field $\vec{b}_o(r)$ which inhibits flow separation for Hartmann numbers $H^2 \geq 2\ R/3^{\frac{1-4}{}}$. The physical reason for this is to be seen in the different nature of the Lorentz force, which is irrotational [$\nabla \times (\vec{j} \times \vec{b}) = \vec{0}$] in the former case and rotational [$\nabla \times (\vec{j} \times \vec{b}) \neq \vec{0}$] in the latter case.

SOLUTION FOR $\psi(\theta)$

For magnetohydrodynamic flows, the magnetic Reynolds number is commonly not large, $R_M \lesssim 1$. For this reason, the eigenvalue problem (29)-(31) for the amplitude $\psi(\theta)$ of the induced magnetic field $B(\rho,\theta)$ can be solved by means of perturbation theory, assuming that $R_M f(\theta)\psi$ is a small term in Eq. (29). Since $f(\theta) \leq f(0) = 1$, this assumption is valid for

$$R_M << \sqrt{\mu_n^{(0)}}, \quad n = 1,2,3,... \quad . \tag{52}$$

In the 0-th approximation, $R_M \to 0$, the eigenvalues and eigenfunctions of Eqs. (29)-(30) are:

$$\mu_n^{(0)} = (n\pi/\theta_o)^2, \qquad n = 1,2,3,... \quad , \tag{53}$$

$$\psi_n^{(0)}(\theta) = c_n \cos(n\pi\theta/\theta_o), \qquad n = 1,2,3,... \quad , \tag{54}$$

with $\psi_n^{(0)}(\theta) = 0$ for $n = 0$ by Eq. (31). For the determination of the eigenvalues and eigenfunctions of the perturbed problem (29)-(31), $R_M > 0$, we set

$$\mu_n = \mu_n^{(0)} + \mu_n^{(1)} + ... \quad , \tag{55}$$

$$\psi_n(\theta) = \psi_n^{(0)}(\theta) + \sum_{\nu=1}^{\infty} a_{\nu n}^{(1)} \psi_\nu^{(0)}(\theta) + ... \quad , \tag{56}$$

in accordance with 1-st order perturbation theory. Substitution of Eqs. (55)-(56) into Eq. (29) yields in the same approximation

$$-\sqrt{\mu_n^{(0)}}\, R_M f(\theta)\, \psi_n^{(0)} + \sum_{\nu=1}^{\infty} a_{\nu n}^{(1)}\, \mu_\nu^{(0)}\, \psi_\nu^{(0)} + ... = \mu_n^{(1)}\, \psi_n^{(0)} + \mu_n^{(0)} \sum_{\nu=1}^{\infty} a_{\nu n}^{(1)}\, \psi_\nu^{(0)} + ... \tag{57}$$

since the terms of 0-th order drop out. Multiplication of Eq. (57) by

$\psi_n^{(0)}$ and integration over $(-\theta_o, +\theta_o)$ yields for the perturbation of the eigenvalues

$$\mu_n^{(1)} = -R_M(n\pi/\theta_o) \int_{-\theta_o}^{+\theta_o} \cos^2(n\pi\theta/\theta_o) f(\theta) d(\theta/\theta_o) \quad , \quad (58)$$

upon consideration of Eqs. (53)-(54). Multiplication of Eq. (57) by $\psi_\nu^{(0)}$, $\nu \neq n$, and integration over $(-\theta_o, +\theta_o)$ yields for the expansion coefficients of 1-st order

$$a_{\nu n}^{(1)} = \frac{R_M(n\pi/\theta_o)}{(\nu\pi/\theta_o)^2-(n\pi/\theta_o)^2} \frac{C_n}{C_\nu} \int_{-\theta_o}^{+\theta_o} \cos(\nu\pi\theta/\theta_o)\, f(\theta)\cos(n\pi\theta/\theta_o) d(\theta/\theta_o)$$

$$, \quad (59)$$

upon consideration of Eqs. (53)-(54). Combining of Eqs. (58)-(59) and (55)-(56) yields for the eigenvalues and eigenfunctions of Eqs. (29)-(31):

$$\mu_n = (n\pi/\theta_o)[(n\pi/\theta_o) - R_M \int_{-1}^{+1} \cos^2 n\pi x\, f(x)\, dx], \; n = 1,2,3,\ldots \quad , \quad (60)$$

$$\psi_n(\theta)/R_M I(\rho_1^{-\sqrt{\mu_n}} - \rho_2^{-\sqrt{\mu_n}})^{-1} =$$

$$\frac{[\cos(n\pi\theta/\theta_o)+R_M(n\pi/\theta_o) \sum_{\nu=1}^{\infty}{}' \; b_{\nu n}\cos(n\pi\theta/\theta_o)]}{[(-1)^n+R_M(n\pi/\theta_o) \sum_{\nu=1}^{\infty}{}' \; (-1)^\nu \, b_{\nu n}]} \quad , \; n=1,2,3,\ldots \quad , \quad (61)$$

where

$$b_{\nu n} = \int_{-1}^{+1} \cos\nu\pi x \; f(x) \; \cos n\pi x \; dx/[(\nu\pi/\theta_o)^2-(n\pi/\theta_o)^2] \quad . \quad (62)$$

In Eqs. (60)-(62), $x = \theta/\theta_o$ as previously, and the expansion coefficients c_n have been determined in Eq. (61) by means of Eq. (31). The parameter m, which determines the radial decay of the induced magnetic

field $B(\rho,\theta) = \rho^{-m}\,\psi(\theta)$, is obtained from μ_n,

$$m \equiv m_n = \sqrt{\mu_n}\,, \quad n = 1,2,3,... \qquad . \quad (63)$$

Since an infinite number "n" of eigenfunctions $\psi_n(\theta)$ exists mathematically, the solution for the induced magnetic field, $B(\rho,\theta) = \rho^{-m(n)}\,\psi_n(\theta)$, is not unique. Probably, only the eigenfunction with n=1 is physically stable, and can be observed in actual diffuser flows across an axial, homogeneous, external magnetic field. A similar non-uniqueness exists for the velocity field $U(\rho,\theta) = f(\theta)/\rho$ of the Hamel flow[7]. For one and the same flow rate $Q > 0$ and duct angle θ_o, up to an infinite number of eigenfunctions $f(\theta)$ exist mathematically, which represent pure outflow ($f>0$), symmetrical mixed out- and inflows ($f\gtrless 0$), and asymmetrical flows ($f\gtrless 0$)[7]. The solution for $f(\theta)$ established above is only insofar "unique" as we have excluded all types of mixed flows ($f\lesseqgtr 0$) for given values of $Q > 0$ and θ_o by means of physical arguments.

In Table I, the first few (n=1,2,3) eigenvalues m_n are compared with their values $m_n^{(0)}$ in the 0-th approximation for $\theta_o = 5^o$, $\alpha = -1/3$, 5, and $R_M = 10^{-2}$, 10^{-1}, 10^0 based on Eqs. (60) and (63). It is obvious that m_n differs hardly from $m_n^{(0)}$ and varies very little with α and R_M, as long as $R_M \ll n\pi/\theta_o$.

TABLE I: Eigenvalues $m_n = \mu_n^{1/2}$, n = 1,2,3($\theta_o=5^o$).

	α=-1/3			α=5			
	$R=10^{-2}$	$R=10^{-1}$	$R=10^{0}$	$R=10^{-2}$	$R=10^{-1}$	$R=10^{0}$	n : $m_n^{(0)}$
m_1	35.9976	35.9760	35.7589	35.9969	35.9694	35.6927	1 : 36.0000
m_2	71.9977	71.9770	71.7695	71.9968	71.9675	71.6748	2 : 72.0000
m_3	107.9977	107.9770	107.7696	107.9967	107.9672	107.6717	3 : 108.0000

Figs. 5 and 6 show the first few (n=1,2,3) eigenfunctions $\psi_n(x)/R_M I$ versus $x = \theta/\theta_o$ for $\alpha = -1/3$, $R_M = 10^o$ and $\alpha = 5$, $R_M = 10^{-2}$, respectively. In both cases, it is assumed that $\theta_o = 5^o$ and $\rho_1 = 1$ ($r_1 = r_o$) and $\rho_2 = 100$($r_2 = 100 r_o$). It is recognized that $\psi_n(x)$ varies little with α and R_M, and that $\psi_n(x) \tilde{=} \psi_n^{(0)}(x)$.

Thus, a homogeneous, external magnetic field $\vec{b}_o$ in the axial direction has the following effects on the radial flow in a diffuser with electrodes in the planes $\theta = \pm\theta_o$. The radial motion of the conducting fluid across $\vec{b}_o$ induces radial, $J_\rho(\rho,\theta)$, and azimuthal, $J_\theta(\rho,\theta)$, current densities. While the net radial current flow due to $J_\rho(\rho,\theta)$ is zero [Eq. (32)], the net azimuthal current flow due to $J_\theta(\rho,\theta)$ is $I \neq 0$ [Eq. (12)] if the external circuit is closed. $J_\theta(\rho,\theta) = mR_M^{-1}\rho^{-(m+1)}\psi_n(\theta)$ changes its direction at those coordinate values θ where $J_\rho(\rho,\theta) = R_M^{-1}\,\rho^{-(m+1)}\,d\psi_n(\theta)/d\theta$ assumes an extremum [Eqs. (15), (21), (61)] as illustrated in Figs. 5-6. The external, $\vec{b}_o$, and induced, $\vec{B}(\rho,\theta)$, magnetic fields in the axial direction produce an irrotational Lorentz force, which changes the pressure distribution in the flow [Eq. (25)], but has no direct influence on the onset of flow separation [Eq. (51)].

The selfsimilar solutions derived are based on the assumption that the flow is two-dimensional (r,θ), which requires a quasi-infinite extension of the flow in the z-direction. Whether the selfsimilar solutions are realistic enough remains to be shown by comparison with actual magnetohydrodynamic diffuser flow experiments, since the condition of similarity may impose restrictions on the generality of the solutions obtained.

The radial, two-dimensional diffuser flow considered represents an idealization which is analogous to the fully developed, axial

Hagen-Poiseuille flow between parallel walls. For a more realistic theory, hydrodynamic and electromagnetic end-effects would have to be considered, as well as z-dependence of the flow fields due to insulating walls in the planes $z = \pm z_o$, $z_o < \infty$. These complications would render it extremely difficult to find selfsimilar solutions, presumed that similarity transformations exist in the three-dimensional case at all.

Citations

1. H. E. Wilhelm, Can. J. Phys. 50, 2327 (1972).
2. S. H. Choi and H. E. Wilhelm, Phys. Fluids 20, 1821 (1977).
3. H. E. Wilhelm and S. H. Choi, Phys. Rev. 16A, 2135 (1977).
4. H. E. Wilhelm, Phys. Fluids 17, 360 (1974).
5. N. Liron and H. E. Wilhelm, Z. angew. Math. Mech. 56, 479 (1976).
6. S. N. Brown and K. Stewardson, Q. J. Mech. appl. Math. 29, 325 (1976).
7. K. Millsaps and K. Pohlhausen, J. Aeron. Sci. 20, 187 (1953).
8. G. W. Sutton and A. Sherman, Engineering Magnetohydrodynamics (McGraw-Hill , New York, 1965).
9. M. Abramowitz and I. Stegun, Handbook of Mathematical Functions (Dover, New York, 1965).
10. H. Schlichting, Boundary Layer Theory (McGraw-Hill, New York 1960).

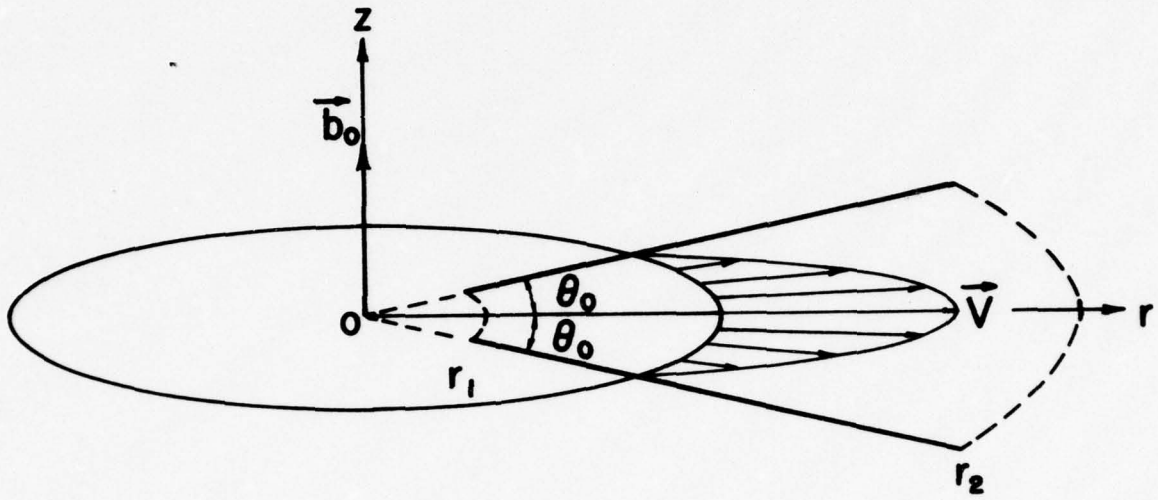

Fig. 1: Geometry of diffuser flow with axial magnetic field $\vec{b}_o$ and radial velocity field $\vec{v}(r,\theta)$.

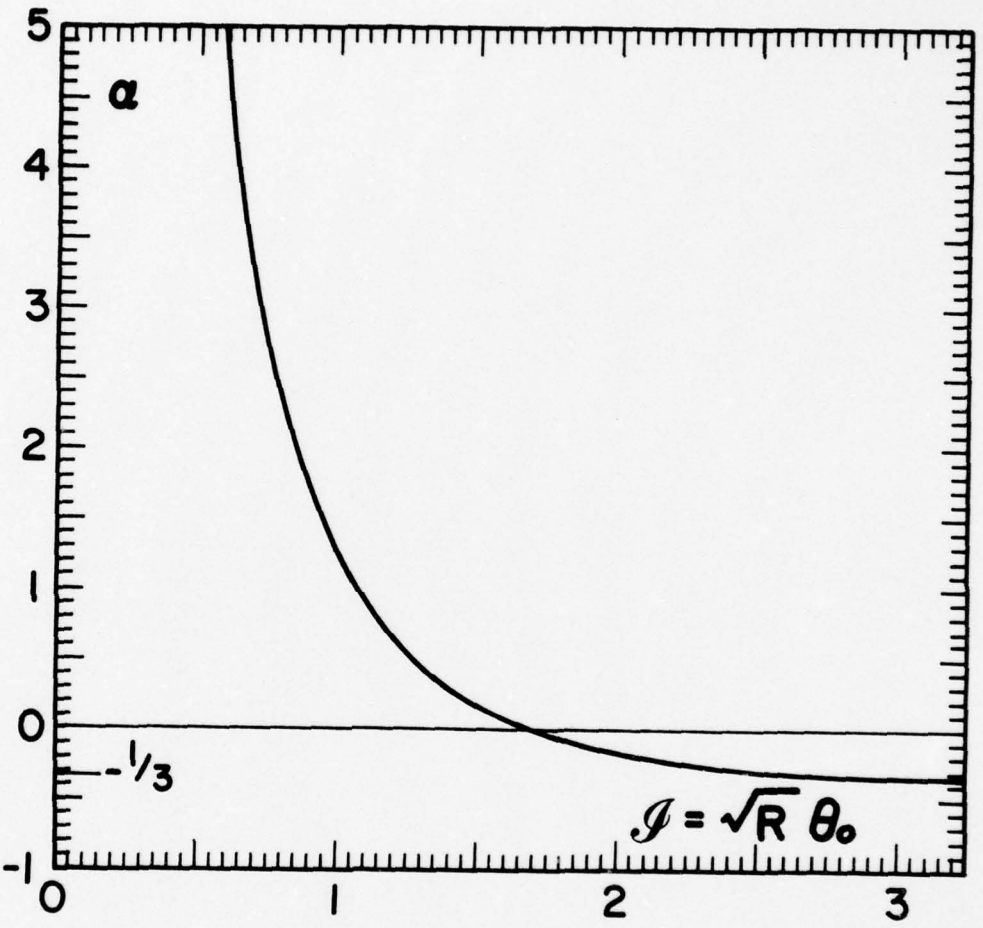

Fig. 2: Eigenvalue α versus invariance parameter $I = R^{\frac{1}{2}}\,\theta_o$.

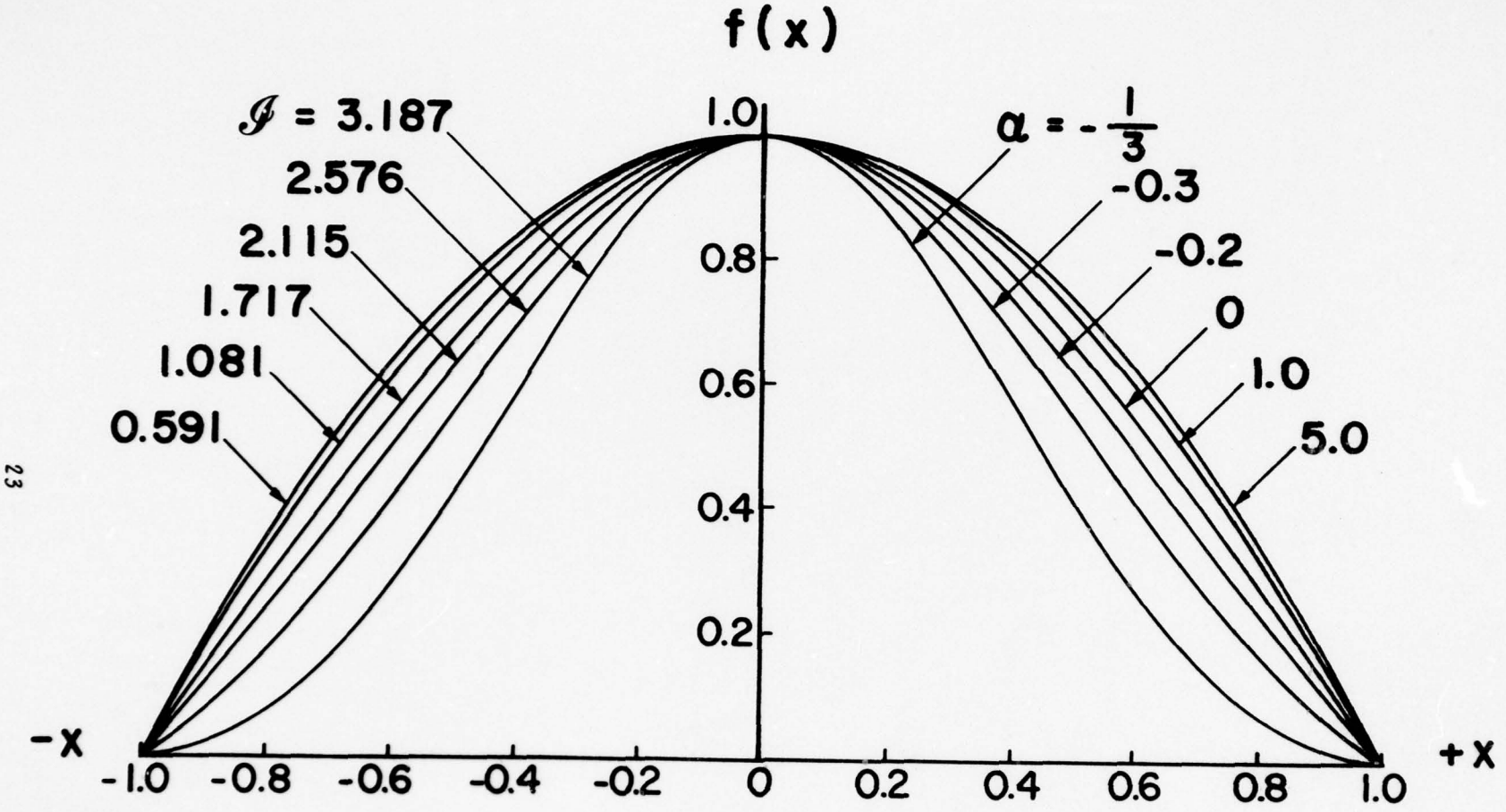

Fig. 3: Velocity amplitude f(x) versus $x = \theta/\theta_o$ for various $I \equiv R^{\frac{1}{2}} \theta_o$.

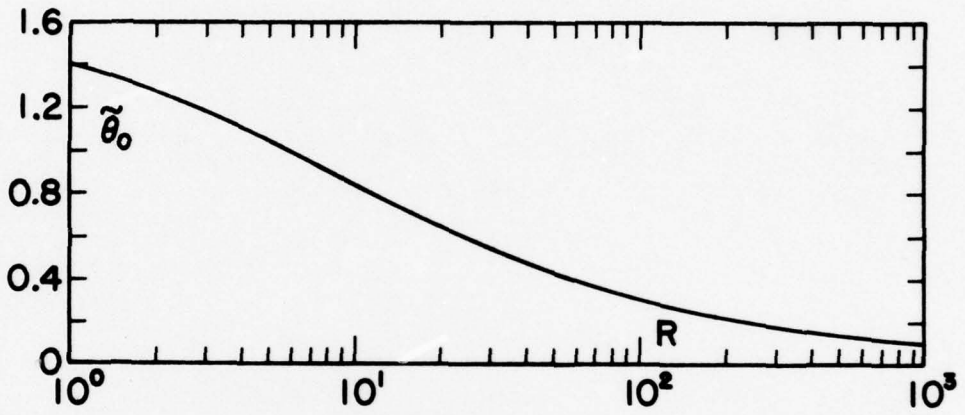

Fig. 4: Critical duct angle $\tilde{\theta}_o$ for separation versus R.

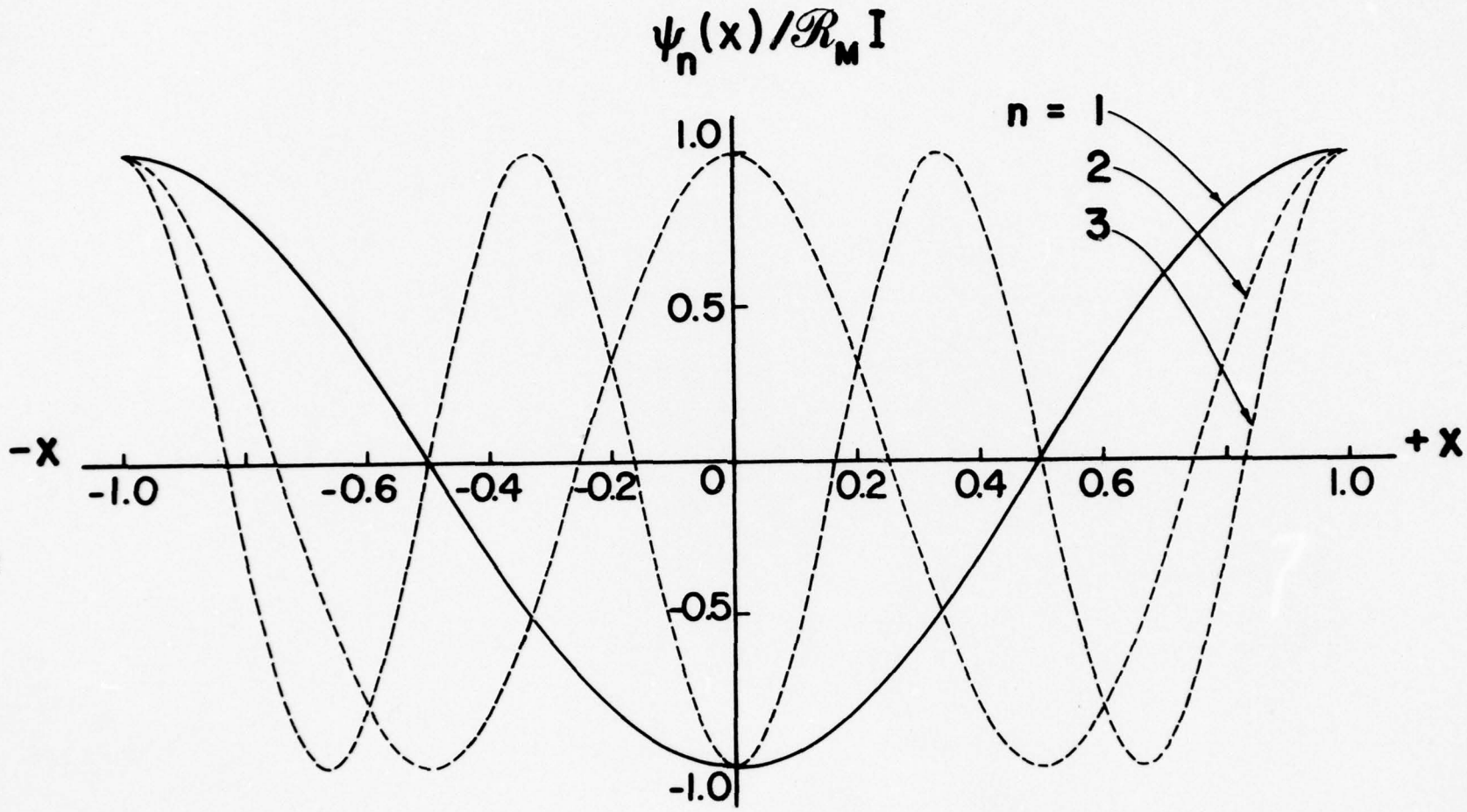

Fig. 5: Magnetic field amplitude $\psi_n(x)$ versus $x = \theta/\theta_o$ for $\alpha = -1/3$, $R_M = 10^{-2}$, $\theta_o = 5^o$, and $n = 1,2,3$.

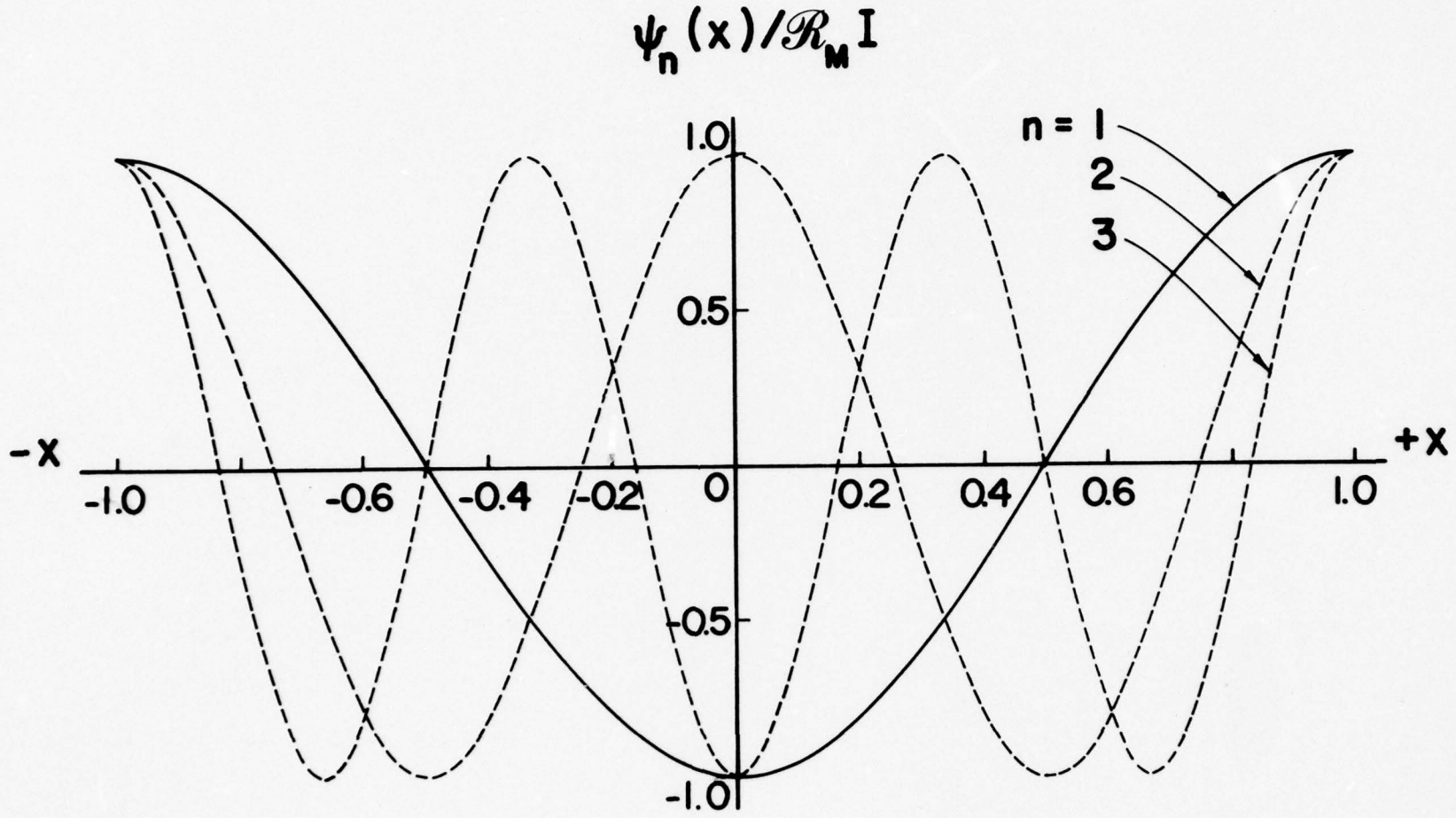

Fig. 6: Magnetic field amplitude $\psi_n(x)$ versus $x = \theta/\theta_o$ for $\alpha = 5$, $R_M = 10^0$, $\theta_o = 5^o$, and $n = 1,2,3$.

Similarity analysis of magnetohydrodynamic flows with viscous stress relaxation

H. E. Wilhelm and S. H. Choi
Department of Electrical Engineering, Colorado State University, Fort Collins, Colorado 80523
(Received 1 March 1977)

A novel similarity solution in terms of a hyperelliptic integral is given for a magnetohydrodynamic flow across an azimuthal magnetic field in a diverging duct, under consideration of viscous stress relaxation. Velocity profiles and the critical duct angle for flow separation are calculated as a function of the Reynolds number and the Hartmann number. It is shown that viscous stress relaxation modifies the velocity distribution and reduces considerably the critical duct angle for flow separation at low Reynolds numbers. At large Reynolds numbers, viscous stress relaxation is less important, and the results approach asymptotically those of ordinary magnetofluiddynamics, which is based on a static relation between viscous stresses and the velocity component gradients.

I. INTRODUCTION

In classical fluid mechanics[1] and magnetohydrodynamics,[2] it is assumed that inhomogeneities $\nabla_i v_j$ in the velocity components v_j produce instantaneously viscous stresses Π_{ij}. Mathematically, this is expressed through a phenomenological "flux"-"force" relation, given for incompressible fluids or subsonic flows by[1,2]

$$\Pi_{ij} = -\mu(\nabla_i v_j + \nabla_j v_i).$$

In a real continuum, velocity inhomogeneities do not switch on viscous stresses instantaneously but rather in accordance with a relaxation process of characteristic time τ. Indeed, the moment

$$\Pi_{ij} = m \iiint (c_i c_j - \tfrac{1}{3} c^2 \delta_{ij}) f(\vec{c}, \vec{r}, t) d^3\vec{c}$$

of the Boltzmann equation yields, for an incompressible viscous fluid ($\nabla \cdot \vec{v} = 0$), the relaxation equation (discussed in connection with the 13-moment approximation in the Appendix):

$$\partial_t \Pi_{ij} + v_k \nabla_k \Pi_{ij} = -\tau^{-1} \Pi_{ij} - p(\nabla_i v_j + \nabla_j v_i),$$

if thermal forces and terms of higher order in the field derivatives are neglected. The viscosity μ, the fluid pressure p, and the viscous stress relaxation time τ are interrelated by $\mu = p\tau$. This equation satisfies the basic requirements of a (classical) $\vec{r}, t$-dependent field equation since it (i) contains space and time derivatives, and (ii) is invariant against Galilei transformation. The static Navier-Stokes relation is not in accordance with either requirement.

The third equation is in the typical form of an inhomogeneous relaxation equation, with a forcing term, $-p(\nabla_i v_j + \nabla_j v_i)$. It is seen that it reduces to the first equation if the temporal ($\partial_t \Pi_{ij}$) and convective ($v_k \nabla_k \Pi_{ij}$) relaxation terms are disregarded.

According to the first equation, viscous stresses would propagate in accordance with a (parabolic) diffusion equation (continuous "signals" and infinite speed of propagation). According to the third equation, viscous stresses would propagate in accordance with a (hyperbolic) wave equation (discontinuous "signal" and finite speed of propagation). This is readily shown, e.g., by combining the equation of motion for the viscous fluid with the first and third stress transport equations, respectively, for the case of a small one-dimensional velocity perturbation. Thus, these equations give rise to a qualitatively significant different behavior in viscous stress transport. Quantitatively, the term $\partial_t \Pi_{ij}$ is of importance for short processes with a duration time $t \leq \tau = \mu/p$. A criterion for the quantitative significance of the term $v_k \nabla_k \Pi_{ij}$ is not as easily establishable, since $\nabla_k \Pi_{ij}$ may be quasisingular at certain points of the fluid. Similarly, the rigorous theory of heat transport has to be based on a (hyperbolic) wave equation.[3]

We consider herein subsonic flows of dense, ionized gases across an external azimuthal magnetic field $\vec{B}_0$ in a duct with inclined walls (so-called diffuser, Fig. 1). The analysis is based on the magnetohydrodynamic equations with viscous-stress relaxation, i.e., we disregard effects of "magnetic" viscosity (which occur in highly rarefied plasma flows) assuming that $\omega_i \tau_i \ll 1$, where $\omega_i = e_i B_0/m_i$ and τ_i are the gyration frequency and collision time of the ions, respectively. By means of an exact (nonlinear) similarity solution, we demonstrate that convective-stress relaxation affects the onset of flow separation, i.e., the first occurrence of wall back flows which, in general, are unstable and result in a turbulent boundary layer. Flow separation is commonly observed if for given Reynolds (R) and Hartmann ($\mathcal{H}$) numbers, the duct angle θ_0 is increased beyond a

critical value θ_0^*. The calculated velocity distributions are qualitatively in agreement with velocity profiles observed in diffusers.[4]

Magnetohydrodynamic diffusers with transverse magnetic fields and nonvanishing electric load are frequently used to study the transformation of kinetic flow energy (due to thermal expansion) into electric energy. For the experimental realization, it is suitable to install the diffuser in a similar larger diverging duct through which the working fluid is pumped at a constant rate in order to minimize three-dimensional entrance effects. The development of the boundary-layer with entrance effect is a complex problem which has been analyzed only for magnetohydrodynamic flows between noninclined walls by means of Goertler series expansions.[5]

II. NONLINEAR BOUNDARY-VALUE PROBLEM

Let cylindrical coordinates (r, θ, z) be introduced for the description of the magnetohydrodynamic flow model (Fig. 1). The conducting fluid is bounded in the surfaces $(\theta = +\theta_0, r_1 \le r \le r_2)$ and $(\theta = -\theta_0, r_1 \le r \le r_2)$ by insulating walls, and in the surfaces $(z = +z_\infty)$ and $(z = -z_\infty)$ by electrodes, which are connected through an ideal circuit $(R = 0)$. The conducting fluid is injected through the inner cylinder section $(r = r_1, -\theta_0 \le \theta \le +\theta_0, -z_\infty \le z \le +z_\infty)$ and removed downstream through the outer cylinder section $(r = r_2, -\theta_0 \le \theta \le +\theta_0, -z_\infty \le \theta \le +z_\infty)$. The boundary layers at the electrodes are disregarded compared with those at the insulating walls by assuming that the interelectrode spacing is large, $z_\infty \gg \frac{1}{2}(r_1 + r_2)\theta_0$. The magnetic field has its sources in an electric current I flowing through a conducting rod $(0 \le r \le r_0, -\infty \le z \le +\infty, r_0 < r_1)$. In accordance with Stokes's law, $\oint \vec{B} \cdot d\vec{s} = \mu_0 I$, the magnetic field is azimuthal (μ_0 is the permeability of vacuum) and has the induction

$$\vec{B} = (\mu_0/2\pi)(I/r)\vec{e}_\theta, \quad r_0 \le r < \infty.$$

The radial flow $\vec{v} = u\vec{e}_r$ of the conducting fluid across the magnetic field $\vec{B}$ induces axial electric (E_z) and current density (j_z) fields, presuming

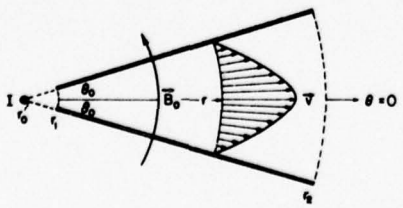

FIG. 1. Geometry of diverging duct with radial velocity field $\vec{v}$ and azimuthal magnetic field $\vec{B}_0$.

that the Hall effect is negligible $(\omega_e \tau_e \ll 1)$,

$$\vec{j} = \sigma(E_z + uB_\theta)\vec{e}_z.$$

The resulting Lorentz force density is a purely radial field which opposes the inducting flow,

$$\vec{j} \times \vec{B} = -\sigma(E_z + uB_\theta)B_\theta \vec{e}_r.$$

Because of $\nabla \times \vec{E} = \vec{0}$ and $\nabla \cdot \vec{j} = \sigma(\nabla \cdot \vec{E} + \vec{B} \cdot \nabla \times \vec{v} - \vec{v} \cdot \nabla \times \vec{B}) = \sigma \nabla \cdot \vec{E} = 0$, the axial electric field is inhomogeneous, and vanishes,

$$\vec{E} = E_z \vec{e}_z = \vec{0}, \quad R = 0,$$

since the load of the external circuit is zero. In this case, the current in the external circuit assumes the maximum value

$$J = \sigma \int_{r_1}^{r_2} \int_{-\theta_0}^{+\theta_0} uB_\theta r \, dr \, d\theta.$$

These equations are based on the assumption that the induced magnetic field is small compared with the external magnetic field, which implies small magnetic Reynolds numbers,[5]

$$R_B = \mu_0 \sigma u(r, 0) r \ll 1.$$

In this elementary radial-flow model, fluid dynamic and electric end effects at $r = r_1$ and $r = r_2 (|\theta| \le \theta_0)$ are disregarded.

The magnetohydrodynamic diffuser flow under consideration is described by the nonlinear boundary-value problem for the radial velocity $[u = u(r, \theta)]$, stress $[\Pi_{ij} = \Pi_{ij}(r, \theta)]$, and pressure $[p = p(r, \theta)]$ fields:

$$\rho u \frac{\partial u}{\partial r} = -\frac{\partial p}{\partial r} - \left(\frac{1}{r}\frac{\partial}{\partial r}(r\Pi_{rr}) + \frac{1}{r}\frac{\partial \Pi_{\theta r}}{\partial \theta} - \frac{\Pi_{\theta\theta}}{r}\right) - \sigma B_\theta^2(r_0)\left(\frac{r_0}{r}\right)^2 u, \tag{1}$$

$$0 = -\frac{1}{r}\frac{\partial p}{\partial \theta} - \left(\frac{1}{r^2}\frac{\partial}{\partial r}(r^2\Pi_{\theta r}) + \frac{1}{r}\frac{\partial \Pi_{\theta\theta}}{\partial \theta}\right), \tag{2}$$

$$\frac{\partial u}{\partial r} + \frac{u}{r} = 0, \tag{3}$$

where

$$\mu \frac{u}{p}\frac{\partial \Pi_{rr}}{\partial r} + \Pi_{rr} = -2\mu \frac{\partial u}{\partial r}, \tag{4}$$

$$\mu \frac{u}{p}\frac{\partial \Pi_{\theta r}}{\partial r} + \Pi_{\theta r} = -\mu \frac{1}{r}\frac{\partial u}{\partial \theta}, \tag{5}$$

$$\mu \frac{u}{p}\frac{\partial \Pi_{\theta\theta}}{\partial r} + \Pi_{\theta\theta} = -2\mu \frac{u}{r}, \tag{6}$$

and

$$u(r, \theta = \pm\theta_0) = 0, \tag{7}$$

$$\rho \int_{-\theta_0}^{+\theta_0} u(r, \theta) r \, d\theta = Q. \tag{8}$$

Equation (8) specifies the flow rate Q through the diverging duct. For similarity reasons, Eq. (8) is equivalent to inlet ($r = r_1$) and outlet ($r = r_2$) boundary conditions. Instead of Eq. (8), it is more convenient to assume the Reynolds number $R(0)$ of the central streamline to be given,[6]

$$\rho u(r, \theta = 0) r/\mu = R(0). \tag{9}$$

Equations (1), (2) are the r and θ components of the equation of motion of the conducting fluid in the azimuthal magnetic field $[B_\theta = B_\theta(r_0) r_0/r]$. Equation (3) represents the continuity equation for incompressible radial flow, and Eqs. (4)–(6) describe the convective stress relaxation with a viscosity $\mu = p\tau$. It is noted that for pure radial flow

$$\vec{v} \cdot \nabla \vec{\Pi} = u \partial \vec{\Pi}/\partial r.$$

III. SIMILARITY TRANSFORMATION

The dimensions of the flow fields and the fluid constants are interrelated by

$$(u) = (\mu/\rho r), \quad (p) = (\Pi_{ij}) = (\mu^2/\rho r^2).$$

Accordingly, we try to reduce the partial Eqs. (1)–(6) into ordinary differential equations by means of the similarity transformation:

$$u(r, \theta) = (\mu/\rho) r^{-1} f(\theta), \tag{10}$$

$$p(r, \theta) = (2\mu^2/\rho) r^{-2} P(\theta), \tag{11}$$

$$\Pi_{rr}(r, \theta) = (2\mu^2/\rho) r^{-2} g_{rr}(\theta), \tag{12}$$

$$\Pi_{\theta r}(r, \theta) = (2\mu^2/\rho) r^{-2} g_{\theta r}(\theta), \tag{13}$$

$$\Pi_{\theta\theta}(r, \theta) = (2\mu^2/\rho) r^{-2} g_{\theta\theta}(\theta). \tag{14}$$

The functions $f(\theta)$, $P(\theta)$, and $g_{ij}(\theta)$ are nondimensional. Upon substitution of Eqs. (10)–(14), we obtain from Eqs. (1)–(9) the ordinary boundary-value problem:

$$f^2 = -4P + 2g'_{\theta r} + \mathcal{K}^2 f, \tag{15}$$

$$P = P_0 - g_{\theta\theta}, \tag{16}$$

$$[(P - f)/P]\, g_{rr} = f, \tag{17}$$

$$[(P - f)/P]\, g_{\theta r} = -\tfrac{1}{2} f', \tag{18}$$

$$[(P - f)/P]\, g_{\theta\theta} = -f, \tag{19}$$

where

$$f(\theta = \pm\theta_0) = 0, \tag{20}$$

$$\int_{-\theta_0}^{+\theta_0} f(\theta)\, d\theta = Q/\mu, \tag{21}$$

and

$$P_0 = P(\theta = \pm\theta_0), \quad f(0) = R(0), \tag{22}$$

$$\mathcal{K}^2 = \left(\frac{\sigma}{\mu}\right) B_\theta^2(r) r^2 = (\sigma/\mu)(\mu_0 I/2\pi)^2. \tag{23}$$

From the stress-relaxation Eqs. (17)–(18) one obtains the conventional static stress relations for $P \gg |f|$: $g_{rr} = -f$, $g_{\theta r} = -\frac{1}{2} f'$, $g_{\theta\theta} = -f$; $P \gg |f|$.

IV. CLOSED-FORM SOLUTION

Substitution of Eq. (16) into Eq. (19) gives the pressure function $P(\theta)$ in terms of the velocity function $f(\theta)$,

$$P = \tfrac{1}{2}[2f + P_0 + (4f^2 + P_0^2)^{1/2}]. \tag{24}$$

The minus sign of the square root is not applicable as one verifies by means of Eqs. (20) and (22). By eliminating $P(\theta)$ by means of Eq. (16) and $g'_{\theta r}$ by means of Eq. (18), we find from Eqs. (15) and (20) the nonlinear boundary-value problem for the velocity function $f(\theta)$,

$$f''[2f + P_0 + (4f^2 + P_0^2)^{1/2}] + 2P_0(4f^2 + P_0^2)^{-1/2} f'^2 + [P_0 + (4f^2 + P_0^2)^{1/2}]\{f^2 + (4 - \mathcal{K}^2) f + 2[P_0 + (4f^2 + P_0^2)^{1/2}]\} = 0, \tag{25}$$

where

$$f(\theta = \pm\theta_0) = 0. \tag{26}$$

The differential equation for the corresponding flow without stress relaxation[7] is obtained from Eq. (15) as

$$f'' + f^2 + (4 - \mathcal{K}^2) f + 4P_0 = 0 \text{ for } P \gg |f|.$$

The substitution,

$$\frac{df}{d\theta} = \psi, \quad \frac{d^2 f}{d\theta^2} = \frac{1}{2}\frac{d\psi^2}{df}, \tag{27}$$

transforms Eq. (25) into a nonlinear differential equation of first order for $\psi = \psi(f)$,

$$\frac{d}{df}\psi^2 + F(f)\psi^2 + G(f) = 0, \tag{28}$$

where

$$F(f) \equiv 4P_0\{[2f + P_0 + (4f^2 + P_0^2)^{1/2}](4f^2 + P_0^2)^{1/2}\}^{-1} > 0, \tag{29}$$

$$G(f) \equiv 2[P_0 + (4f^2 + P_0^2)^{1/2}] \times \{f^2 + (4 - \mathcal{K}^2) f + 2[P_0 + (4f^2 + P_0^2)^{1/2}]\} \times [2f + P_0 + (4f^2 + P_0^2)^{1/2}]^{-1} \gtrless 0. \tag{30}$$

The general solution of Eq. (28) is found by the method of variation of the integration constant of the solution of the associated homogeneous equation as

$$\psi^2(f) = \exp\left(-\int_{f_0}^{f} F(f)\,df\right) \times\left[\psi_0^2 - \int_{f_0}^{f} \exp\left(+\int_{f_0}^{f} F(f)\,df\right) G(f)\,df\right], \quad (31)$$

$f_0 \equiv f(0)$,
where

$$\psi_0 \equiv \psi(f = f(0)) = \left(\frac{df}{d\theta}\right)_{\theta=0} = 0 \quad (32)$$

for symmetrical flows. Combining of Eqs. (27) and (31) yields an integral solution for $\theta = \theta(f)$ from which one obtains the analytical solution $f = f(\theta)$ by inversion

$$\pm\theta = \int_{f_0}^{f(\theta)} H^{-1}(f)\,df, \quad f_0 \equiv f(0), \quad (33)$$

where

$$H(f) = \left\{\exp\left(-\int_{f_0}^{f} F(f)\,df\right) \times\left[\psi_0^2 - \int_{f_0}^{f} \exp\left(+\int_{f_0}^{f} F(f)\,df\right) G(f)\,df\right]\right\}^{1/2}. \quad (34)$$

Equations (33) and (34) represent a closed-form solution for the magnetohydrodynamic diffuser flow with viscous stress relaxation in terms of a hyperelliptic integral, since by Eq. (34),

$$H^2(f) = \frac{[P_0 + (4f^2 + P_0^2)^{1/2}]}{[2f + (4f^2 + P_0^2)^{1/2}]}\left(\frac{[2f_0 + (4f_0^2 + P_0^2)^{1/2}]}{[P_0 + (4f_0^2 + P_0^2)^{1/2}]}\psi_0^2 - \tfrac{1}{2}(\tfrac{2}{3}(f^3 - f_0^3) + \tfrac{1}{2}(16 - 2\mathcal{K}^2 - P_0)(f^2 - f_0^2) + P_0\mathcal{K}^2(f - f_0) + \tfrac{1}{12}[(4f^2 + P_0^2)^{3/2} - (4f_0^2 + P_0^2)^{3/2}] + \tfrac{1}{2}(8 - \mathcal{K}^2)[f(4f^2 + P_0^2)^{1/2} - f_0(4f_0^2 + P_0^2)^{1/2}] + \tfrac{1}{4}(8 - \mathcal{K}^2)P_0^2\{\ln[2f + (4f^2 + P_0^2)^{1/2}] - \ln[2f_0 + (4f_0^2 + P_0^2)^{1/2}]\}\right). \quad (35)$$

In Eq. (33), the ± sign has to be used depending on whether $df/d\theta \gtrless 0$, or $\theta \lesseqgtr 0$ in case of pure outflows, $f(\theta) > 0$. The integration constant ψ_0 is determined in Eq. (32) for symmetrical flows with an extremum at $\theta = 0$, which are of main practical interest. The remaining integration constant P_0 contained in the solution of Eq. (33) is determined by the boundary condition in Eq. (26), which gives

$$\theta_0 = \int_0^{f_0} H^{-1}(f)\,df. \quad (36)$$

Based on Eqs. (33)–(36), velocity distributions $f(\theta) \gtrless 0$ of pure outflows have been computed for the typical duct angle $\theta_0 = 5^0$ and given Reynolds numbers $R \equiv R(0) = f(0)$ of the central stream line $\theta = 0$, with the Hartmann number $\mathcal{K}$ as parameter, $\mathcal{K}^2 \gtrless 0.7R > \frac{2}{3}R$. In the presence of viscous stress relaxation, the onset of flow separation, as will be shown, is inhibited at large Reynolds numbers R for Hartmann numbers

$$\mathcal{K} > \mathcal{K}_{cr};\ \mathcal{K}_{cr}^2 \cong \tfrac{2}{3}R \text{ for } R \gg 1.$$

The velocity distributions in Figs. 2, 3, and 4 represent net outflows without backflow regions since $\mathcal{K} > \mathcal{K}_{cr}$. Figure 2 shows $f(\theta)$ for the relatively small Reynolds number $R = 10^3$ and $\mathcal{K}^2 = 0.7R - 10\,R(\theta = 5^0)$. The velocity distributions become flatter and the velocity gradients at the walls $\theta = \pm\,\theta_0$ increase in magnitude as $\mathcal{K}$ increases.

Figure 3 shows $f(\theta)$ for the moderate Reynolds number $R = 10^4$ and $\mathcal{K}^2 = 0.7R - 5R(\theta_0 = 5^0)$. In this case, $|df(\theta = \pm\theta_0)/d\theta|$ decreases with decreasing $\mathcal{K}$ so that a well developed flow exists only in the central region for small $\mathcal{K}^2 > \frac{2}{3}R$. Figure 4 shows $f(\theta)$ for the relatively large Reynolds number $R = 10^5$ and $\mathcal{K}^2 = 0.7R - 5R$ $(\theta_0 = 5^0)$. For small Hartmann numbers, $\mathcal{K}^2 > \frac{2}{3}R$, the flow is considerably depressed in the extended regions adjacent to the walls so that Reynolds numbers $R(\theta) \cong 10^5$ are realized only in the limited central section $|\theta| < \frac{1}{10}\theta$ of the duct. The $f(\theta)$ curves in Fig. 4 show clearly the transition to the limiting velocity distribution, for which $|df(\theta = \pm\theta_0)/d\theta|$ assumes the smallest realizable value, as $\mathcal{K} \to \frac{2}{3}R$. It is con-

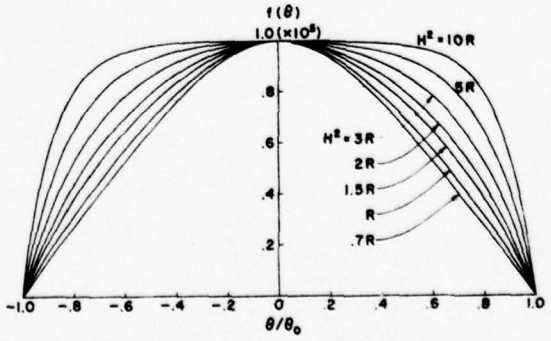

FIG. 2. $f(\theta)$ vs θ for $R = 10^3$ and various $\mathcal{K}$ $(\theta_0 = 5^0)$.

cluded that well developed velocity distributions exist for sufficiently large Hartmann numbers $\mathcal{H}=\mathcal{H}(R;\theta_0)$, e.g., $\mathcal{H}^2>\frac{2}{3}R$ for $R=10^3$ (Fig. 2) and $\mathcal{H}^2\geq 2R$ for $R=10^4$ (Fig. 3) and $R=10^5$ (Fig. 4).

Velocity distributions of the typical form shown in Figs. 3 and 4 have been observed in magnetohydrodynamic diffuser-flow experiments.[4] A qualitative comparison is, however, not possible, since a conical diffuser was used in the experiments.[4] Velocity distributions without stress relaxation have been calculated previously.[8]

V. MAGNETOHYDRODYNAMIC FLOW SEPARATION

The integral solution derived in Eqs. (33), (35), and (36) describes physical flows as long as $P_0 \equiv P(\theta=\pm\theta_0)\geq 0$ for the given parameters R, $\mathcal{H}$, and θ_0, since the pressure field has to be positive everywhere, $P(\theta)\geq 0$, $|\theta|\leq\theta_0$. The boundary-value problem in Eqs. (25)–(26) becomes, in the limiting case $P_0=0$,

$$\tilde{f}''+\tfrac{1}{2}(8-\mathcal{H}^2)\tilde{f}+\tfrac{1}{2}R\tilde{f}^2=0, \tag{37}$$

$$\tilde{f}(\theta=\pm\theta_0)=0, \tag{38}$$

where

$$\tilde{f}(\theta)\equiv\frac{f(\theta)}{f(0)}=\frac{f(\theta)}{R};\quad \tilde{f}(\theta=0)\equiv 1;\quad R\equiv R(0). \tag{39}$$

Since $P_0=0$ in Eq. (37), it cannot be reduced to the relaxation-free case ($P, P_0 \gg f$). The solution for the limiting flow with vanishing wall pressure P_0 is by Eqs. (37)–(38),

$$\pm\theta=(3/R)^{1/2}\int_1^{\tilde{f}(\theta)}\frac{d\tilde{f}}{[-Q(\tilde{f})]^{1/2}}, \tag{40}$$

where

$$Q(\tilde{f})=\tilde{f}^3+\frac{3}{2R}(8-\mathcal{H}^2)\tilde{f}^2-\frac{3}{2R}(8-\mathcal{H}^2)-1 \tag{41}$$

is a trinomial in $\tilde{f}$ which has one real and two complex conjugate roots since, in general,

$2R>8-\mathcal{H}^2$:

$$\tilde{f}_1=1,$$

$$\tilde{f}_{2,3}=\frac{3}{4R}(8-\mathcal{H}^2+\tfrac{2}{3}R)\left[-1\pm i\left(-1+\frac{(\frac{8}{3}R)}{8-\mathcal{H}^2+\frac{2}{3}R}\right)^{1/2}\right]. \tag{42}$$

Equation (40) contains an elliptic integral which is resolved by means of the substitution

$$\tilde{f}(\theta)=1-\lambda^2\left(\frac{1-\cos\phi}{1+\cos\phi}\right),\quad 0\leq\phi\leq\pi \tag{43}$$

which gives

$$\pm\theta=-(3/R)^{1/2}\lambda^{-1}F(\phi,k) \tag{44}$$

where

$$\lambda=\{3[1+(8-\mathcal{H}^2)R^{-1}]\}^{1/4}, \tag{45}$$

$$k^2=\tfrac{1}{2}\{1+\tfrac{3}{4}\lambda^{-2}[2+(8-\mathcal{H}^2)R^{-1}]\}. \tag{46}$$

Inversion of Eq. (44) and substitution of ϕ in Eq. (43) yields the explicit solution for the case $P_0=0$:

$$\tilde{f}(\theta)=1-\lambda^2\frac{1-\mathrm{cn}[(\frac{1}{3}R)^{1/2}\lambda\theta,k]}{1+\mathrm{cn}[(\frac{1}{3}R)^{1/2}\lambda\theta,k]}. \tag{47}$$

According to Eq. (44), the critical duct angle $\theta_0(P_0=0)$ at which the wall pressure is zero is given by the boundary condition $\tilde{f}(\theta=\pm\theta_0)=0$ as,

$$\theta_0(P_0=0)=(3/R)^{1/2}\lambda^{-1}F(\phi_0,k), \tag{48}$$

$$\phi_0=\arccos[(\lambda^2-1)/(\lambda^2+1)], \tag{49}$$

in terms of the characteristic flow numbers R and $\mathcal{H}$ [$\lambda=\lambda(R,\mathcal{H})$, $k=k(R,\mathcal{H})$ by Eqs. (45)–(46)]. Since $f_{2,3}=0$ for $\mathcal{H}^2-8=\frac{2}{3}R$ by Eq. (42), the integral in Eq. (40) diverges for $\tilde{f}(\theta=\pm\theta_0)=0$. Similarly, Eq. (47) diverges in this case since $k\to 1$ for $\mathcal{H}^2-8=\frac{2}{3}R$ by Eq. (46). It is recognized that

$$0\leq\theta_0\leq\theta_0(P_0=0)=\pi \text{ for } \mathcal{H}^2\geq 8+\tfrac{2}{3}R, \tag{50}$$

$$0<\theta_0\leq\theta_0(P_0=0)<\pi \text{ for } \mathcal{H}^2<8+\tfrac{2}{3}R. \tag{51}$$

Accordingly, physical flow solutions with $P(\theta)$

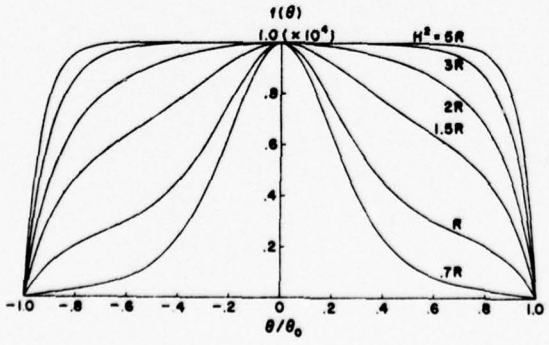

FIG. 3. $f(\theta)$ vs θ for $R=10^4$ and various $\mathcal{H}(\theta_0=5°)$.

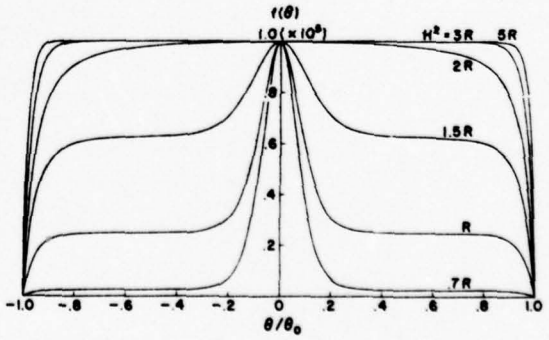

FIG. 4. $f(\theta)$ vs θ for $R=10^5$ and various $\mathcal{H}(\theta_0=5°)$.

$\geq 0, |\theta| \leq \theta_0$, exist for all duct angles $0 < \theta_0 \leq \pi$ if the Hartmann number is

$$\mathcal{H} \geq \mathcal{H}_{cr}, \quad \mathcal{H}_{cr}^2 = 8 + \tfrac{2}{3}R. \tag{52}$$

On the other hand, if $\mathcal{H} < \mathcal{H}_{cr}$, physical flow solutions with $P(\theta) > 0, |\theta| < \theta_0$, exist only for duct angles $\theta_0 > \theta_0(P_0 = 0) < \pi$.

In Fig. 5, the critical duct angle $\theta_0^s = \theta_0(P_0 = 0)$ for vanishing wall pressure is plotted versus $R = R(0)$ with $\mathcal{H}$ as a parameter. It is seen that θ_0^s decreases with increasing R, but increases with increasing $\mathcal{H}$. The stabilizing effect of the magnetic field at sufficiently large Hartmann numbers $\mathcal{H}$ is apparent, in particular, in the regions $\mathcal{H} > \mathcal{H}_{cr}(R)$.

The critical duct angle $\theta_0^s = \theta_0(P_0 = 0)$ is also obtained from the condition $df(\theta = \pm\theta_0)/d\theta = 0$, if viscous-stress relaxation is not taken into consideration.[7] The corresponding curves $\theta_0^s = \theta_0(R, \mathcal{H})$ are shown dashed in Fig. 5. Comparison indicates that for the same R and $\mathcal{H}$, θ_0^s "without stress relaxation" is considerably larger than θ_0^s "with stress relaxation" for relatively small Reynolds numbers, $R < 10^2$. Accordingly, viscous-stress relaxation has a destabilizing effect on the flow, which, however, is completely negligible for large Reynolds numbers, $R \gg 10^2$. As the wall pressure drops to zero, the laminar flow solution can no longer be realized, and flow separation sets in for duct angles $\theta_0 > \theta_0^s(R, \mathcal{H}) < \pi$.

In the classical similarity theory for incompressible viscous flow between inclined walls,[6] solutions with a (positive) homogeneous overpressure p_0 exist so that one does not have to be concerned about negative pressures in back-flow regions at the onset of separation. The similarity analysis of the corresponding compressible flow[8] no longer permits solutions with over pressure, and the limiting flow solution with $df(\theta = \pm\theta_0)/d\theta = 0$ exhibits a negative wall pressure, $P_0 < 0$. For this reason, the onset of separation was determined from the condition $P(\theta = \pm\theta_0) \equiv 0$.[8] Similarly, here we have associated the onset of separation in flows with stress relaxation with the vanishing of the wall pressure, $P_0 = 0$. The observed stabilizing effect of the magnetic field is due to the increase in the wall pressure (Fig. 6) with increasing Hartmann number $\mathcal{H}$. In conventional incompressible fluid dynamics without stress relaxation, the conditions $df(\theta = \pm\theta_0)/d\theta = 0$ and $P(\theta = \pm\theta_0) = 0$ lead to the same separation criterion.

Interest in this theoretical problem arose in connection with experiments on boundary-layer separation in incompressible liquid metal flow and subsonic magnetogasdynamic flow in nonuniform magnetic fields and ducts.[4,9] If the Hartmann number is set to zero, the closed-form solutions presented reduce to those for the flow of electrically nonconducting ordinary fluids with viscous-stress relaxation in diverging ducts.

ACKNOWLEDGMENT

This work was supported in part by the U. S. Office of Naval Research.

APPENDIX: VISCOUS STRESS TRANSPORT EQUATION

Incompressible magnetohydrodynamics is applicable to conducting liquids such as liquid metals, and also, as an approximation, to collision-dominated ionized gases and plasmas at subsonic flow speeds. In each case, the viscous momentum transport is due to the heavy atomic particles while the electrons affect only the stress relaxation time τ through cross-collisions. For this reason, conducting fluids can be described by one-fluid magnetohydrodynamic equations.

The stress-relaxation equation for incompres-

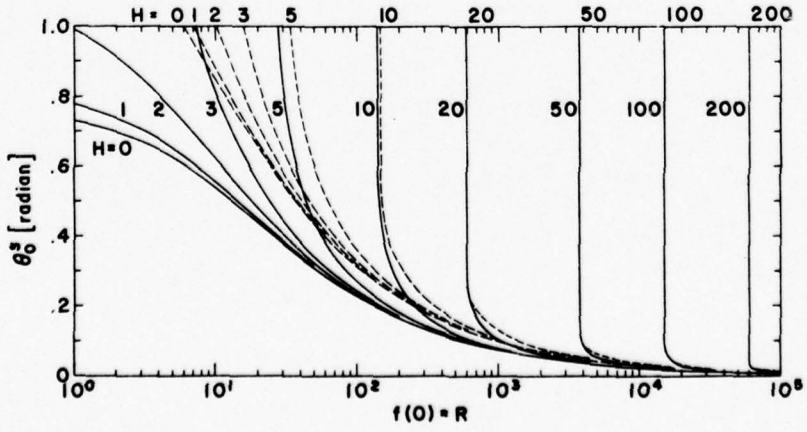

FIG. 5. Critical duct angle θ_0^s for separation vs R for various $\mathcal{H}$, with (——) and without (---) viscous-stress relaxation.

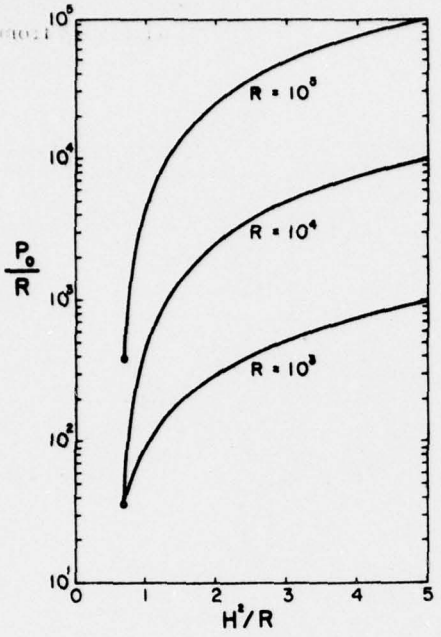

FIG. 6. Wall pressure P_0 vs $\mathcal{H}$ for various R ($\theta_0 \approx 5^0$).

sible ($\nabla \cdot \vec{v} = 0$) flows is derived as a special case of the stress-relaxation equation for compressible ($\nabla \cdot \vec{v} \neq 0$) flows based on the Boltzmann equation presuming that the fluids are sufficiently dense and collision dominated. For liquids a similar stress relaxation equation can be derived from the Born-Green kinetic equation which differs from the Boltzmann equation through the collision integral for many-body collisions. The most elegant method of solution for the Boltzmann equation is the 13-moment approximation due to Grad,[10-12] which is mathematically also more rigorous than the Chapman-Enskog and Hilbert methods.[13] The closure of the 13-moment approximation is forced by truncating the third-order heat-flux tensor Q_{ijk} in terms of the heat-flux vector $\vec{q}$

$$Q_{ijk} \equiv \iiint_{-\infty}^{+\infty} m c_i c_j c_k f(\vec{c}, \vec{r}, t) d^3\vec{c}$$

$$= \tfrac{2}{5}(q_i \delta_{jk} + q_j \delta_{ki} + q_k \delta_{ij}), \qquad \text{(A1)}$$

where $f(\vec{c}, \vec{r}, t)$ is the distribution of thermal velocities $\vec{c}$. This truncation affects mainly the heat-flow dynamics, and is, therefore, an excellent approximation for quasi-isothermal magnetohydrodynamic flows ($\vec{q} = \vec{0}$).

Following the original deduction of Grad for a neutral one-component gas,[10] we multiply the Boltzmann equation for particles of mass m_r and charge e_r in an electromagnetic field $\vec{E} - \vec{B}$ by $\frac{1}{2}m_r[\vec{c}_r\vec{c}_r - (\frac{1}{3})c_r^2\vec{\delta}]$ and integrate it over the entire space $\int\int\int d^3\vec{c}_r$ of the thermal velocities $\vec{c}_r$ of the r particles. Thus, the following moment-conservation equation is obtained for the nonhydrostatic stress tensor $\vec{\Pi}_r = \vec{P}_r - p_r\vec{\delta}$ of the r component (summation s over the remaining components s of the fluid):

$$\frac{\partial}{\partial t}\vec{\Pi}_r + \vec{\Pi}_r \times \vec{\omega}_r + [\vec{\Pi}_r \times \vec{\omega}_r]^{-1} + \vec{v}_r \cdot \nabla\vec{\Pi}_r + \vec{\Pi}_r \nabla \cdot \vec{v}_r + p_r(\nabla\vec{v}_r + [\nabla\vec{v}_r]^{-1} - \tfrac{2}{3}\nabla \cdot \vec{v}_r\vec{\delta}) + \tfrac{2}{5}(\nabla\vec{q}_r + [\nabla\vec{q}_r]^{-1} - \tfrac{2}{3}\nabla \cdot \vec{q}_r\vec{\delta})$$
$$+ (\vec{\Pi}_r \cdot \nabla\vec{v}_r + [\vec{\Pi}_r \cdot \nabla\vec{v}_r]^{-1} - \tfrac{2}{3}\vec{\Pi}_r : \nabla\vec{v}_r\vec{\delta}) = \sum_s \iiint_{-\infty}^{+\infty} m_r[\vec{c}_r\vec{c}_r - \tfrac{1}{3}\vec{c}_r^2\vec{\delta}]C_{rs}\,d\vec{c}_r, \qquad \text{(A2)}$$

where

$$C_{rs} = \int \cdots \int (f_r^* f_s^* - f_r f_s)\sigma_{rs}(g_{rs}, \Omega) g_{rs}\, d\Omega\, d\vec{c}_s \qquad \text{(A3)}$$

is the binary collision integral,[10] and $\vec{\omega}_r = -e_r\vec{B}/m_r$ is the gyration frequency ($[\ ]^{-1}$ designates the inverse tensor). In the 13-moment approximation, the distribution functions $f_r(\vec{c}_r, \vec{r}, t)$ and $f_s(\vec{c}_s, \vec{r}, t)$ are expanded in Hermite tensorial polynomials, the expansion coefficients being the first (scalar) 13 moments of the distribution function.[10] By means of these expansions and Eq. (A3) it can be shown that Eq. (A2) is of the form

$$\frac{\partial\vec{\Pi}_r}{\partial t} + \vec{B}_r = -\tau_r^{-1}\vec{\Pi}_r - \sum_{s \neq r} \alpha_{rs}\tau_{rs}^{-1}\vec{\Pi}_s, \qquad \text{(A4)}$$

where τ_r is the viscous-stress relaxation time[14] and τ_{rs} is the relaxation time describing the linear momentum exchange[14] between the components r and $s \neq r$. $\vec{B}_r$ is an abbreviation for the remaining tensor terms on the left side of Eq. (A2), and α_{rs} are numerical coefficients. For representative times $t \gg \tau_r$, the term $\partial\vec{\Pi}_r/\partial t$ in Eq. (A4) is negligible, and one obtains the quasi-equilibrium, $\vec{\Pi}_r$ proportional to the sum of the various driving force tensors.[10] The tensor $\vec{B}_r$ reduces not always to the velocity gradients $\nabla\vec{v}_r$ of the Navier-Stokes relation,[10] and for representative times $t \lesssim \tau_r$, the 13-moment approximation does not approximate the phenomenological Navier-Stokes relation and gives better results.[10]

For magnetohydrodynamic applications, a sim-

ple-stress transport equation for the electrically conducting, incompressible fluid as a whole can be deduced from Eq. (A2) by neglecting those terms which are small compared with the leading terms. The contribution of the electrons (e) to the fluid of ions (i) and atoms (a) as a whole is insignificant since $m_e \ll m_{i,a}$ and[14] $\alpha_{ei}, \alpha_{ea} \ll 1$. The magnetic anisotropy terms are negligible since $\omega_i \tau_i \ll 1$ for the heavy ions, and vanish for the neutral atoms ($\omega_a = 0$). The $\nabla \cdot \vec{v}_r$ terms can be disregarded for incompressible fluids and subsonic (compressible) flows. The $\vec{q}_r$ terms are negligible for quasi-isothermal flows, and the terms $\vec{\Pi}_r \cdot \nabla \vec{v}_r$ are of the order of magnitude of quadratic terms in $\nabla \vec{v}_r$, and therefore small compared to the linear ones. The stresses in the electron gas have no effect on the stress distribution of the fluid as a whole ($m_e \ll m_{i,a}$). Thus, one obtains from Eq. (A2) as stress transport equation for incompressible, quasi-isothermal fluid as a whole:

$$\partial \vec{\Pi} / \partial t + \vec{v} \cdot \nabla \vec{\Pi} = -\tau^{-1} \vec{\Pi} - p(\nabla \vec{v} + [\nabla \vec{v}]^{-1}), \qquad \text{(A5)}$$

where $\vec{v} = \sum n_r m_r \vec{v}_r / \sum n_r m_r$ is the mean-mass velocity of the fluid. The relaxation frequency τ^{-1} of the total stress tensor $\vec{\Pi}$ is a linear combination of the inverse relaxation times $\tau_i^{-1}, \tau_a^{-1}, \tau_{rs}^{-1}$. The Reynolds number in the preceding similarity analysis and τ are related by $R(0) = [\rho u(0) r / p(0)] \tau^{-1}$.

Equation (A5) can also be derived directly from elementary physical arguments. The Navier-Stokes driving force $-p(\nabla \vec{v} + [\nabla \vec{v}]^{-1})$ of $\vec{\Pi}$ follows from the symmetry argument of Einstein. The term $\partial \vec{\Pi} / \partial t$ results from the fact that the Navier-Stokes quasi-equilibrium $\vec{\Pi} / \tau = -p(\nabla \vec{v} + [\nabla \vec{v}]^{-1})$ develops within a time of the order of the "collision" time τ. Finally, the convective term $\vec{v} \cdot \nabla \vec{\Pi}$ has to be added in order to make Eq. (A5) invariant against Galilei transformations ($\vec{r}' = \vec{r} - \vec{w}t, t' = t$).

We have based the deduction of the stress transport equation on Grad's 13-moment theory, which gives all driving forces (for the viscous stresses) which have a simple physical meaning, i.e., not only the Navier-Stokes forces $\sim \nabla \vec{v}$ and $\sim [\nabla \vec{v}]^{-1}$. It is seen that the 13-moment theory is more comprehensive and more rigorous than the Navier-Stokes theory, and "refuses to predict results which may be inaccurate."[10] On the other hand, the failures of the Navier-Stokes stress equation may assume catastrophic proportions, e.g., it "predicts smooth solutions for shock strengths of infinite magnitude (with a transition from negative to a positive density)."[10]

---

[1] L. D. Landau and E. M. Lifschitz, *Fluid Mechanics* (Addison-Wesley, Reading, Mass., 1968), p. 47.
[2] S. Chandrasekhar, *Hydrodynamic and Hydromagnetic Stability* (University Press, Oxford, 1961), p. 12.
[3] H. E. Wilhelm and S. H. Choi, J. Chem. Phys. 63, 2119 (1975); S. H. Choi and H. E. Wilhelm, Phys. Rev. A 14, 1825 (1976).
[4] I. E. Idel'chik and Ya. L. Ginzburg, Magn. Gidrodin. 6, 148 (1970) [Magnetohydrodynamics 6, 148 (1970)].
[5] A. Sherman, Phys. Fluids 4, 552 (1961).
[6] K. Millsaps and K. Pohlhausen, J. Aeron. Sci. 20, 187 (1953).
[7] H. E. Wilhelm, Can. J. Phys. 50, 2327 (1972).
[8] H. E. Wilhelm, Phys. Fluids 17, 360 (1974).
[9] B. Zauderer, Phys. Fluids 11, 2577 (1968).
[10] H. Grad, *Principles of Kinetic Theory of Gases* (Springer, New York, 1958), HP. 12, 205.
[11] H. Grad, Commun. Pure Appl. Math. 2, 331 (1949).
[12] H. Grad, Commun. Pure Appl. Math. 5, 257 (1952).
[13] H. Grad, Phys. Fluids 6, 147 (1963).
[14] S. Herdan and B. S. Liley, Rev. Mod. Phys. 32, 731 (1960).

Self-similar magnetohydrodynamic diffuser flows with induced magnetic fields

S. H. Choi and H. E. Wilhelm

Department of Electrical Engineering, Colorado State University, Fort Collins, Colorado 80523
(Received 22 February 1977; final manuscript received 11 July 1977)

The steady diffuser flow of a viscous incompressible fluid with a finite electrical conductivity in the presence of an external magnetic field is analyzed by means of similarity theory. Power series expansions for the velocity and induced magnetic fields are presented, and discussed as dependent on the Reynolds, Hartmann, magnetic Reynolds numbers, and duct angle. Short-circuit current and the critical values of magnetic Reynolds number and duct angle for flow separation are calculated. It is shown that the induced magnetic field changes the velocity profile and considerably reduces the critical duct angle at which flow separation occurs. The critical magnetic Reynolds number for flow separation becomes smaller as the Reynolds number increases.

I. INTRODUCTION

Extensions of the Jeffery–Hamel flow theory[1,2] to magnetohydrodynamics have been made by a few authors.[3–6] These approaches to magnetohydrodynamic flows in a diffuser are based on the approximation, (i) that the induced magnetic field is negligible (magnetic Reynolds number $M \ll 1$),[3–6] or (ii) that the working fluid is an ideal electric conductor (electrical conductivity $\sigma \to \infty$).[3]

In the following, the steady flow of an incompressible viscous fluid with finite conductivity between two inclined walls (diffuser) in the presence of azimuthal, external, and induced magnetic fields is analyzed. The electrical conductivity is assumed to be constant throughout the diffuser. This approximation is applicable to conducting liquid and incompressible (subsonic) gaseous plasma flows.[7]

It is shown that the steady motion of the conducting fluid does not induce a magnetic field in the azimuthal direction, but does induce it in the radial direction. An analytical solution to the magnetohydrodynamic flow problem is accomplished by reducing the nonlinear partial differential equations to ordinary ones via a similarity transformation, and solving the latter equations in terms of power series. The magnetohydrodynamic field profiles are presented in dependence of the Reynolds (R), Hartmann (H), magnetic Reynolds (M) numbers, and duct angle (θ_0).

In the limiting case of small magnetic Reynolds numbers ($M \ll 1$), the nonlinear boundary value problem reduces to the conventional magnetohydrodynamic diffuser problem,[4] which is based on the approximation that the induced magnetic field is small compared with the applied magnetic field.

II. PHYSICAL PRINCIPLES

The electrically conducting fluid flows between two nonparallel, insulating walls and two parallel electrode plates as shown in Fig. 1. The electrodes are short-circuited so that there is no potential difference between them. The influence of a load in the external circuit has been investigated previously.[4] The conducting fluid is injected through the inner duct section at $r = r_0$ and removed downstream through the outer duct section at $r = r_1$. The boundary layers at the electrodes are disregarded compared with those at the insulating walls presuming that the inter-electrode spacing is large, $z_\infty \gg \frac{1}{2}(r_0 + r_1)\theta_0$. The external magnetic field has its source in an electric current I_0 flowing through an infinitely long conducting rod located in the z axis. In accordance with Ampere's law, $\oint \mathbf{B} \cdot d\mathbf{s} = \mu_0 I_0$, the external magnetid field is azimuthal and has the induction (μ_0 is the permeability of vacuum),

$$B_0 = (\mu_0/2\pi)(I_0/r) .$$

In the absence of flow sources or sinks at the walls, the velocity field is radial, i.e., $\mathbf{v} = [v(r, \theta), 0, 0]$. The flow of the fluid across the external magnetic field B_0 induces a current density field in the axial direction, $J_z = \sigma(E_z + vB_0)$ presuming that the Hall effect is negligible. A magnetic field B_r is induced in the radial direction by the current density J_z. Since $\nabla \times \mathbf{E} = 0$ and $\nabla \cdot \mathbf{J} = \sigma \nabla \cdot (\mathbf{E} + \mathbf{v} \times \mathbf{B}) = \sigma \nabla \cdot \mathbf{E} = 0$, a homogeneous electric field $\mathbf{E}$ is possible. However, $E_z = 0$, since the terminal voltage is zero due to the short-circuited external circuit, and $E_{r,\theta} = 0$ since the boundary conditions for $E_{r,\theta}$ are homogeneous. The Hall effect is assumed to be negligible, $\omega\tau \ll 1$ ($\omega = eB/m$ is the gyration frequency and τ is the collision time of the electrons). Thus, Maxwell's equa-

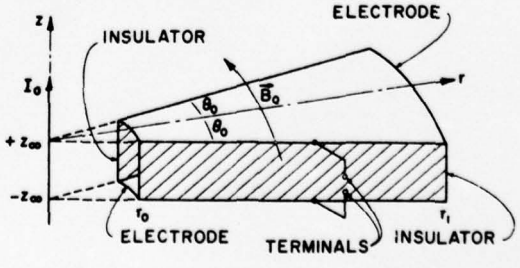

FIG. 1. Diffuser duct geometry.

Copyright © 1977 American Institute of Physics

tions and Ohm's law give, for the magnetic field $\mathbf{B} = (B_r, B_\theta, 0)$, the induction equation,

$$\nabla \times \mathbf{B}/\mu_0 \sigma = \mathbf{v} \times \mathbf{B} .$$

III. BOUNDARY VALUE PROBLEM

In nondimensional form, indicated by the overbars, the radial velocity $\bar{v}(\bar{r}, \theta)$, the pressure $\bar{p}(\bar{r}, \theta)$, and the magnetic field $\bar{B} = [\bar{B}_r(\bar{r}, \theta), \bar{B}_\theta(\bar{r}, \theta), 0]$ are described by the nonlinear boundary-value problem:

$$\frac{1}{\bar{r}} \frac{\partial}{\partial \bar{r}} (\bar{r}\bar{v}) = 0 , \tag{1}$$

$$\bar{v} \frac{\partial \bar{v}}{\partial \bar{r}} = - \frac{\partial \bar{p}}{\partial \bar{r}} + \frac{1}{R} \left[\frac{\partial^2 \bar{v}}{\partial \bar{r}^2} + \frac{1}{\bar{r}} \frac{\partial \bar{v}}{\partial \bar{r}} + \frac{1}{\bar{r}^2} \frac{\partial^2 \bar{v}}{\partial \theta^2} - \frac{\bar{v}}{\bar{r}^2} \right] - \frac{H^2}{R} \frac{1}{M} \left[\frac{1}{\bar{r}} \frac{\partial}{\partial \bar{r}} (\bar{r}\bar{B}_\theta) - \frac{1}{\bar{r}} \frac{\partial \bar{B}_r}{\partial \theta} \right] \bar{B}_\theta , \tag{2}$$

$$0 = - \frac{1}{\bar{r}} \frac{\partial \bar{p}}{\partial \theta} + \frac{2}{R} \frac{1}{\bar{r}^2} \frac{\partial \bar{v}}{\partial \theta} + \frac{H^2}{R} \frac{1}{M} \frac{1}{\bar{r}} \left[\frac{\partial}{\partial \bar{r}} (\bar{r}\bar{B}_\theta) - \frac{\partial \bar{B}_r}{\partial \theta} \right] \bar{B}_r , \tag{3}$$

$$\frac{1}{M} \left[\frac{1}{\bar{r}} \frac{\partial}{\partial \bar{r}} (\bar{r}\bar{B}_\theta) - \frac{1}{\bar{r}} \frac{\partial \bar{B}_r}{\partial \theta} \right] = \bar{v}\bar{B}_\theta , \tag{4}$$

$$\frac{1}{\bar{r}} \frac{\partial}{\partial \bar{r}} (\bar{r}\bar{B}_r) + \frac{1}{\bar{r}} \frac{\partial \bar{B}_\theta}{\partial \theta} = 0 . \tag{5}$$

In Eqs. (1)–(5), the Reynolds (R), Hartmann (H), and magnetic Reynolds (M) numbers, and the dimensionless variables are defined by

$$R = \frac{v_0 r_0}{(\mu/\rho_0)} , \quad H^2 = \left(\frac{\sigma}{\mu} \right) \left(\frac{\mu_0 I_0}{2\pi} \right)^2 , \quad M = \sigma \mu_0 v_0 r_0 , \tag{6}$$

and

$$\bar{v} = v/v_0 , \quad \bar{p} = p/\rho_0 v_0^2 , \quad \bar{B}_\theta = B_\theta/(\mu_0 I_0/2\pi r_0) ,$$
$$\bar{B}_r = B_r/(\mu_0 I_0/2\pi r_0) , \quad \bar{r} = r/r_0 , \tag{7}$$

where v_0 is the input velocity at $r = r_0$, and $\theta = 0$ (central stream line). The solutions to Eqs. (1)–(5) are subject to the following conditions:

$$\bar{v}(\bar{r}, \pm\theta_0) = 0 , \tag{8}$$

$$\bar{B}_\theta(\bar{r}, \pm\theta_0) = \bar{B}_0(\bar{r}) , \tag{9}$$

$$\bar{v}(\bar{r}, +\theta) = \bar{v}(\bar{r}, -\theta) \geq 0 , \tag{10}$$

$$\bar{B}_r(\bar{r}, +\theta) = - \bar{B}_r(\bar{r}, -\theta) , \tag{11}$$

$$\frac{Q}{\rho_0 v_0 r_0} = \int_{-\theta_0}^{+\theta_0} \bar{v}\bar{r}\, d\theta . \tag{12}$$

Equation (8) contains the boundary conditions for no slip of $\bar{v}(\bar{r}, \theta)$ at the walls. Equation (9) considers the continuity of the normal component B_θ at the wall interfaces $[\bar{B}_0(\bar{r}) = 1/\bar{r}]$. Equations (10) and (11) represent the symmetry condition for $\bar{v}(\bar{r}, \theta)$ and the asymmetry condition for $\bar{B}_r(\bar{r}, \theta)$, respectively [Eq. (11) will be justified later]. Equation (12) gives the flow rate Q per unit depth ($\Delta z = 1$).

IV. SIMILARITY TRANSFORMATION AND SERIES EXPANSIONS

The continuity equation (1) indicates that the velocity field is of the self-similar form

$$\bar{v}(\bar{r}, \theta) = F(\theta)/\bar{r} . \tag{13}$$

For dimensional reasons, the pressure and magnetic induction fields are written as

$$\bar{p}(\bar{r}, \theta) = G(\theta)/\bar{r}^2 , \tag{14}$$

$$\bar{B}_r(\bar{r}, \theta) = \psi(\theta)/\bar{r} , \tag{15}$$

$$\bar{B}_\theta(\bar{r}, \theta) = (1/\bar{r})[1 + \phi(\theta)] . \tag{16}$$

In Eq. (16), $\phi/\bar{r}$ represents the induced magnetic field in the azimuthal direction, and $1/\bar{r}$ is the external field.

Substitution of Eqs. (15) and (16) into Eq. (5) (continuity equation for $\mathbf{B}$) gives

$$d\phi/d\theta = 0 . \tag{17}$$

Hence,

$$\phi(\theta) = \text{const} \equiv 0, \text{ and } \bar{B}_\theta = 1/\bar{r} \tag{18}$$

by Eq. (9). Thus, the azimuthal component of magnetic induction is not affected by the steady motion of the conducting fluid. Substitution of Eqs. (13), (14), (15), and (18) into Eqs. (1)–(5) yields the coupled nonlinear ordinary differential equations:

$$- F^2 = 2G + \frac{1}{R} \frac{d^2F}{d\theta^2} + \frac{H^2}{R} \frac{1}{M} \frac{d\psi}{d\theta} , \tag{19}$$

$$\frac{d}{d\theta} \left(G - \frac{2}{R} F + \frac{H^2}{2R} \frac{1}{M} \psi^2 \right) = 0 , \tag{20}$$

$$- \frac{1}{M} \frac{d\psi}{d\theta} = F , \tag{21}$$

where

$$F(\theta = \pm\theta_0) = 0 , \quad F(+\theta) = F(-\theta) \geq 0 , \tag{22}$$

$$\psi(+\theta) = - \psi(-\theta) , \tag{23}$$

and

$$\int_{-\theta_0}^{+\theta_0} F\, d\theta = \frac{1}{R} \frac{Q}{\mu} . \tag{24}$$

Since the velocity field is symmetrical and greater than zero for pure outflow $[F(+\theta) = F(-\theta) \geq 0]$, $d\psi/d\theta \leq 0$ everywhere and $\psi(+\theta) = - \psi(-\theta)$ by Eq. (21). Thus, the condition in Eq. (23), or Eq. (11) is justified.

Integration of Eq. (20) with respect to θ yields

$$G = \frac{2}{R} F - \frac{H^2}{2R} \frac{1}{M} \psi^2 + g_0 , \tag{25}$$

where g_0 is an integration constant. In the limit of large Reynolds number R, $G(\theta)$ in Eq. (25) becomes the constant g_0, i.e., the pressure field would no longer depend on the transverse coordinate (θ) (in agreement with the so-called boundary-layer approximation[8]).

Elimination of $G(\theta)$ in Eq. (19) by means of Eq. (25) leads to

$$\frac{d^2F}{d\theta^2} + RF^2 + 4F + \frac{H^2}{M} \left(\frac{d\psi}{d\theta} - \psi^2 \right) + C_0 = 0 , \tag{26}$$

where $C_0 \equiv 2Rg_0$ is an integration constant proportional to g_0. Hence, the problem reduces to solving two coupled nonlinear differential equations [Eqs. (21) and (26)].

In the limiting case of vanishing induced magnetic

TABLE I. Integration constant $C_0 \equiv 2R$ go for $R = 10^4$, $M = 1$, $\theta_0 = 5°$, and various H.

H^2	C_0
$2R$	1.0101×10^4
$3R$	2.0004×10^4
$5R$	3.9999×10^4
$10R$	8.9999×10^4

field ($M \to 0$), by eliminating $d\psi/d\theta$ in Eq. (26) by means of Eq. (21) and taking $\psi(\theta) \to 0$ and $F(\theta) \to f(\theta)/R$, Eq. (26) reduces to the equation, $f'' + (4 - H^2)f + f^3 + \alpha = 0$, which has been solved in closed form in terms of elliptic functions.[4]

Normalizing $\psi(\theta)$ by the factor M,

$$\Psi(\theta) = \psi(\theta)/M \ , \tag{27}$$

and eliminating $F(\theta)$ from Eq. (26) by means of Eq. (21), one obtains a single nonlinear inhomogeneous differential equation for $\Psi(\theta)$

$$\frac{d^3\Psi}{d\theta^3} - R\left(\frac{d\Psi}{d\theta}\right)^2 + (4 - H^2)\frac{d\Psi}{d\theta} + MH^2\Psi^2 = C_0 \ . \tag{28}$$

By Eqs. (21) and (27), the conditions in Eq. (22) and (23) reduce to

$$\Psi(0) = 0 \ , \tag{29}$$

$$d\Psi(\pm\theta_0)/d\theta = 0 \ , \tag{30}$$

$$d^2\Psi(0)/d\theta^2 = 0 \ . \tag{31}$$

The flow rate is given by

$$\frac{Q}{\mu R} = \int_{-\theta_0}^{+\theta_0} F\, d\theta = -\int_{-\theta_0}^{+\theta_0}\left(\frac{d\Psi}{d\theta}\right)d\theta = \mp 2\Psi(\pm\theta_0) \ ,$$

i.e.,

$$Q = \mp 2\mu R\Psi(\pm\theta_0) \ . \tag{32}$$

Equation (32) could be used as a boundary condition for $\Psi(\theta)$ presuming that the flow rate Q is given (R would then no longer be independent). It is, however, mathematically more convenient to assume the Reynolds number $R(0)$ of the central streamline to be given by[9]

$$R \equiv R(0) = \rho_0 v(r, \theta = 0) r/\mu \ , \tag{33}$$

which implies

$$F(\theta = 0) = 1 \ . \tag{34}$$

The solution $\Psi(\theta)$ of Eq. (28) can be expanded in terms of a power series with respect to θ, which satisfies the conditions in Eqs. (29) and (31)

$$\Psi(\theta) = \sum_{n=0}^{\infty} a_{2n+1}\theta^{2n+1} \ . \tag{35}$$

The equivalent condition to Eq. (34) is, by Eqs. (21) and (27),

$$d\Psi/d\theta = -1 \ \text{ at } \theta = 0 \ . \tag{36}$$

Equation (36) determines the first power coefficient in Eq. (35),

$$a_1 = -1 \ . \tag{37}$$

Substitution of Eq. (35) into Eq. (28) gives

$$\begin{aligned}
a_3 &= \tfrac{1}{6}[C_0 + Ra_1^2 - (4 - H^2)a_1] \ , \\
a_5 &= \tfrac{1}{60}[6Ra_1a_3 - 3(4 - H^2)a_3 - MH^2a_1^2] \ , \\
a_7 &= \tfrac{1}{840}[R(10a_1a_5 + 9a_3^2) - 5(4 - H^2)a_5 - 2MH^2a_1a_3] \ , \\
a_9 &= \tfrac{1}{504}[R(14a_1a_7 + 30a_3a_5) - 7(4 - H^2)a_7 \\
&\quad - MH^2(2a_1a_5 + a_3^2)] \ , \\
&\cdots \\
&\cdots \ ,
\end{aligned} \tag{38}$$

$$\begin{aligned}
a_{2n+1} = \frac{1}{2n(4n^2-1)}\Big[&C_0\,\delta_{1n} - (2n-1)(4-H^2)a_{2n-1} \\
&+ R\sum_{k=0}^{k=n-1}(2k+1)(2n-2k-1)a_{2k+1}a_{2n-2k-1} \\
&- MH^2\sum_{k=0}^{k=n-2}a_{2k+1}a_{2n-2k-3}\Big] \ , \quad n = 1, 2, 3, \ldots \ ,
\end{aligned} \tag{39}$$

where $\delta_{1n} = 1$ for $n = 1$ and $\delta_{1n} = 0$ for $n \neq 1$. Equation (39) is a two-term recurrence relation from which for a given a_{2n+1} one can readily compute a_{2n+3} and then a_{2n+5}, a_{2n+7}, and so on, as far as desired.

The nondimensional functions $\Psi(\theta)$ and $F(\theta) = -\Psi'(\theta)$ are, by Eqs. (35) and (37),

$$\Psi(\theta) = -\theta + \sum_{n=1}^{\infty} a_{2n+1}\theta^{2n+1} \ , \tag{40}$$

$$F(\theta) = 1 - \sum_{n=1}^{\infty}(2n+1)a_{2n+1}\theta^{2n} \ . \tag{41}$$

The condition in Eq. (30) determines the integration constant C_0 in Eq. (39),

$$1 = \sum_{n=1}^{\infty}(2n+1)a_{2n+1}\theta_0^{2n} \ , \quad a_{2n+1} = a_{2n+1}(C_0) \ . \tag{42}$$

Equation (42) is a function of C_0 for a given duct angle θ_0. By Eqs. (25) and (27), the pressure field $G(\theta)$ is, in terms of $\Psi(\theta)$ given by ($C_0 \equiv 2Rg_0$),

$$G(\theta) = [2F(\theta) - MH^2\Psi^2(\theta)/2 + C_0/2] \ . \tag{43}$$

Equations (39)–(43) represent the formal mathematical *resolution of the boundary-value problem* under consideration.

V. DISCUSSION AND RESULTS

Based on a numerical iteration of Eq. (42), the values of the integration constant C_0 are given for various Reynolds (R), Hartmann (H), and magnetic Reynolds (M) numbers in Tables I and II.

A. Flow fields

In Fig. 2, the nondimensional velocity amplitude $F(\theta)$ is shown for $R = 10^4$, $M = 1$, $\theta_0 = 5°$, and various values of H. The width of the boundary layer is considerably reduced as the Hartmann number H increases. The influence of the magnetic Reynolds number M on the velocity profiles is exhibited for $R = 10^3$, 10^5, and $H^2 = 3R$, $\theta_0 = 5°$ in Figs. 3 and 4, respectively. It is seen that the velocity distribution becomes flatter in the center, but the boundary-layer width remains almost constant

TABLE II. Integration constant $C_0 \equiv 2Rg_0$ for $H^2 = 3R$, $\theta_0 = 5°$, and various M

M \ R	10^3	10^4	10^5
1	2.1226×10^3	2.0004×10^4	2.0000×10^5
10	2.1416×10^3	2.0055×10^4	2.0006×10^5
20	2.1620×10^3	2.0107×10^4	2.0012×10^5
24.6			2.0014×10^5
30	2.1819×10^3	2.0157×10^4	
42.6		2.0215×10^4	
50	2.2201×10^3		
222.87	2.4987×10^3		

as M decreases. The velocity profiles for the critical magnetic Reynolds numbers, above which flow separation occurs, are plotted with a dotted line in Figs. 3 and 4.

In Figs. 5 and 6, the nondimensional induced magnetic field amplitude $\Psi(\theta)[\equiv \psi(\theta)/M]$ is shown for $R = 10^3$, 10^5 with $H^2 = 3R$ and $\theta_0 = 5°$, respectively. In these figures, $\Psi(\theta)$ increases in magnitude from the center to the walls for M less than a certain critical value, for which flow separation sets in. $\Psi(\theta)$ for the critical magnetic Reynolds number is plotted with dotted line. Unless M is of the order of unity or larger, it is seen that $\psi(=M\Psi)$ is small compared with the applied field. In pure outflows, the induced magnetic field does not vanish at the walls since the net current flow across the diffuser in the axial direction is nonzero.

In accordance with Eqs. (6), (7), (13), and (18), the axial current density is

$$J_z = \sigma v B_\theta = (I_0/2\pi r_0^2)\, MF(\theta)/\bar{r}^2 \tag{44}$$

in dimensional form, or in dimensionless form

$$\bar{J}_z = MF(\theta)/\bar{r}^2 , \tag{45}$$

where $\bar{J}_z = J_z/(I_0/2\pi r_0^2)$. For pure outflows, the current flows everywhere in the same direction as I_0 since $F(\theta) \geq 0$ in Eq. (45). From Eq. (44), the short-circuit current flowing across the electrodes is

$$I_{sc} = \int_{r_0}^{r_1}\int_{-\theta_0}^{+\theta_0} J_z\, r\, d\theta\, dr = \left(\frac{MI_0}{2\pi}\right)\ln\left(\frac{r_1}{r_0}\right)\int_{-\theta_0}^{+\theta_0} F(\theta)\, d\theta , \tag{46}$$

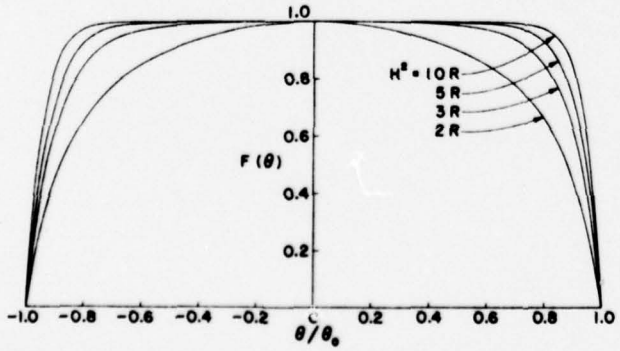

FIG. 2. $F(\theta)$ versus θ for $R = 10^4$, $M = 1$, $\theta_0 = 5°$, and various H.

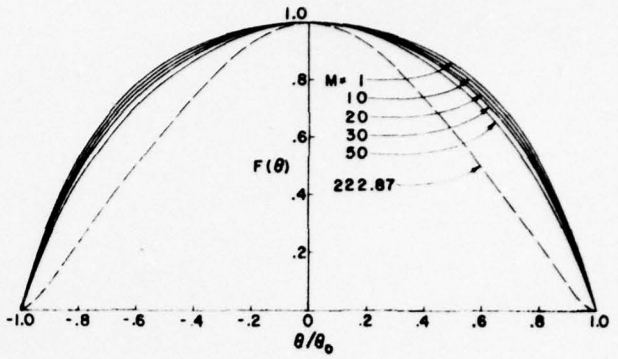

FIG. 3. $F(\theta)$ versus θ for $R = 10^3$, $H^2 = 3R$, $\theta_0 = 5°$, and various M. $\bar{J}_z$ is proportional to $F(\theta)$.

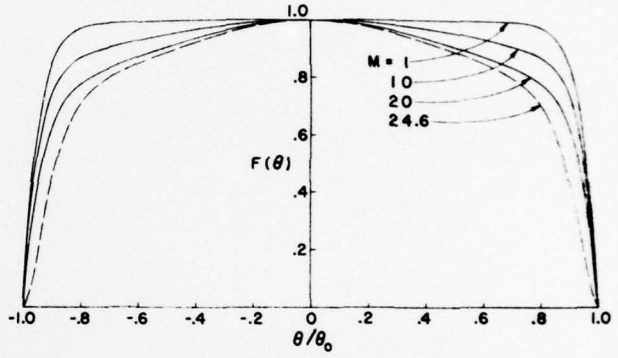

FIG. 4. $F(\theta)$ versus θ for $R = 10^5$, $H^2 = 3R$, $\theta_0 = 5°$, and various M. $\bar{J}_z$ is proportional to $F(\theta)$.

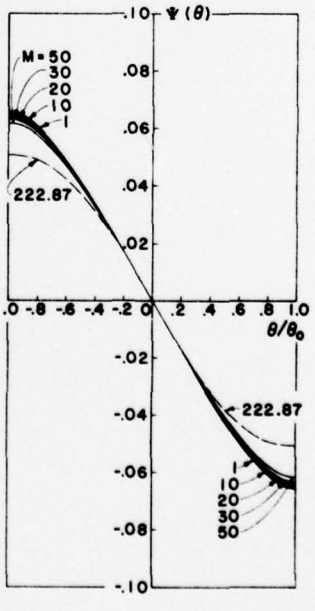

FIG. 5. $\Psi(\theta)$ versus θ for $R = 10^3$, $H^2 = 3R$, $\theta_0 = 5°$, and various M. $\bar{I}_{sc}$ is equal to $M\,|\,\Psi(\pm\theta_0)\,|$.

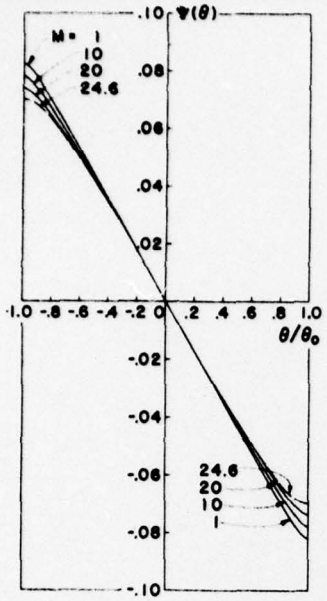

FIG. 6. $\Psi(\theta)$ versus θ for $R = 10^5$, $H^2 = 3R$, $\theta_0 = 5°$, and various M. $\bar{I}_{sc}$ is equal to $M|\Psi(\pm\theta_0)|$.

or in terms of the flow rate,

$$\bar{I}_{sc} = (M/R)\,\bar{Q}\ln(r_1/r_0)\ , \tag{47}$$

where $\bar{I}_{sc} = I_{sc}/(I_0/2\pi)$ and $\bar{Q} = Q/\mu = R\int_{-\theta_0}^{+\theta_0} F(\theta)\,d\theta$. In accordance with Eq. (32), the flow rate is given in terms of $\Psi(\pm\theta_0)$,

$$\bar{I}_{sc} = M\,|\Psi(\pm\theta_0)|\ln(r_1/r_0)^2\ . \tag{48}$$

Thus, the axial current density in Eq. (45) and net short-circuit current in Eq. (48) can be visualized for various R, H, and M numbers with $\theta_0 = 5°$ in Figs. 3, 4 and 5, 6, respectively. An additional illustration for $\bar{I}_{sc}$ is given in Fig. 7 as a function of M for various values of H.

B. Flow separation

Magnetohydrodynamic flow separation sets in if one of the flow parameters goes beyond its "critical" value, e.g., if the duct angle θ_0 is larger than a critical value, $\theta_c = \theta_0(R, H, M)$. If R, H, and M are assumed to be given, θ_c cannot be chosen independently since it assumes the role of an eigenvalue.

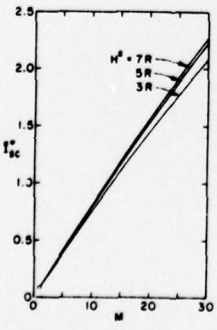

FIG. 7. $\bar{I}^*_{sc}$ [$\equiv \bar{I}_{sc}/M\ln(r_1/r_0)^2$] versus M for various H.

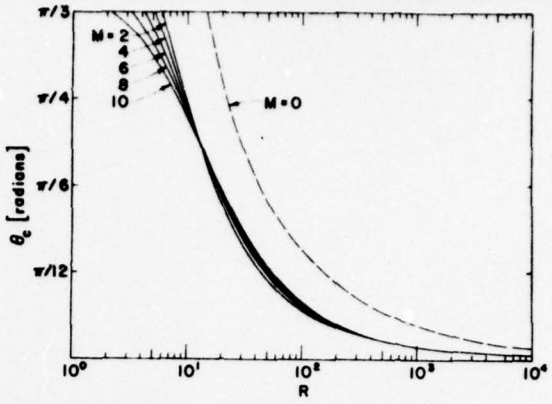

FIG. 8. The critical duct angle θ_c for flow separation versus R for $H = 3$ and various M, with (——) and without (- - -) induced magnetic induction.

The power series solution derived in Eqs. (40), (41), and (43) describes physical flows as long as $G_w = G(\theta = \pm\theta_0) \geq 0$ for any set of parameters R, H, M, and θ_0, since the pressure field has to be positive everywhere, i.e., $G(\theta) \geq 0$, $|\theta| \leq \theta_0$. Since $F(\theta) = 0$ at the walls, G_w in Eq. (43), which is related to the wall pressure, is given by

$$G_w = (C_0 - MH^2\Psi^2_{\theta=\pm\theta_0})/2R\ . \tag{49}$$

As the pressure field drops to zero at the walls, the laminar flow can no longer be realized, so that flow separation occurs for duct angles larger than a critical duct angle θ_c at which separation first sets in.[8] Hence, at the onset of separation, Eq. (49) yields

$$C_0 = MH^2\Psi^2_{\theta=\pm\theta_c}\ . \tag{50}$$

For the limiting flow of vanishing wall pressure, Eq. (50) reduces Eqs. (40) and (41) to

$$-(C_0/MH^2)^{1/2} = -\theta_c + \sum_{n=1}^{\infty} a_{2n+1}\,\theta_c^{2n+1}\ , \tag{51}$$

and

$$1 = \sum_{n=1}^{\infty}(2n+1)\,a_{2n+1}\,\theta_c^{2n}\ , \tag{52}$$

where $a_{2n+1} = a_{2n+1}(C_0)$. The critical duct angle $\theta_c = \theta_0(R, M, H)$ is, therefore, obtained by solving the two coupled equations, (51) and (52), numerically. In Fig. 8, the critical duct angles are plotted as a function of R for various values of M and a given H. It is seen that θ_c decreases as R increases. As M increases, the critical duct angle θ_c decreases for low Reynolds numbers ($R \lesssim 10$) and increases for intermediate Reynolds numbers ($10 \lesssim R \lesssim 10^3$), while θ_c varies little with $M > 1$ at high Reynolds numbers ($R \gtrsim 10^3$). The critical duct angle θ_c for the limiting case of vanishing induced magnetic field ($M \to 0$)[4] is shown with a dashed line in Fig. 8. Comparison indicates that the induced magnetic field reduces the critical duct angle by about 50%.

A simple way of simulating the self-similar flow injection is to put the diverging channel with free entrance and exit openings into a larger, similar duct through

which the conducting fluid is pumped. This method is commonly used in experiments on ordinary, nonconducting Hamel flows between inclined walls.[10]

ACKNOWLEDGMENT

This research was supported in part by the U. S. Office of Naval Research.

[1]G. B. Jeffery, Philos. Mag. **29**, 455 (1915).
[2]G. Hamel, Jber. Dtsch. Mat. Ver. **25**, 34 (1916).
[3]A. B. Vatazhin, J. Appl. Math. Mech. **24**, 765 (1960).
[4]H. E. Wilhelm, Can. J. Phys. **50**, 2327 (1972).
[5]H. E. Wilhelm, Phys. Fluids, **17**, 360 (1974).
[6]H. E. Wilhelm and S. H. Choi, Phys. Rev. A **16**, 1724 (1977).
[7]G. W. Sutton and A. Sherman, *Engineering Magnetohydrodynamics* (McGraw-Hill, New York, 1965), Chap. 10.
[8]H. Schlichting, *Boundary-Layer Theory* (McGraw-Hill, New York, 1968), Chap. VII.
[9]K. Millsaps and K. Pohlhausen, J. Aeronaut, Sci. **20**, 187 (1953).
[10]J. Nikuradse, Ver. Dtsch. Ing. A **281**, 1 (1926); Z. Angew. Math. Mech. **8**, 424 (1928).

Reprinted from Journal of APPLIED PHYSICS Vol. 48, No. 9, September 1977

Stark effect in three-dimensional stochastic electric fields and a static magnetic field of a helium plasma[a]

S. H. Kim

Department of Nuclear Engineering, Hanyang University, Seoul 133, Korea
(Received 14 December 1976; accepted for publication 18 April 1977)

Atomic absorption spectra of the He I plasma in the static magnetic field in the absence of laser radiation are different from spectra in the presence of laser radiation. Especially, it has been theoretically predicted that the spectral shift of the satellite line, which is seen in the latter case, does not exist in the former case. In this paper, the effect of three-dimensional high-frequency electric fields on the σ_+, σ_-, and π components of the allowed 1^1S_0-3^1P_1 transition and the forbidden 1^1S_0-3^1D_2 lines in atomic absorption spectra of the He I plasma in a static magnetic field in the absence of a laser beam is investigated from the coupled equations for the probability amplitudes of atomic states. It is shown that they should give rise to a spectral shift of the allowed lines and satellites about forbidden lines. The calculation reveals that the shift is proportional to the mean-square stochastic electric field, and that the ratio of the intensity of the near satellite to that of the far satellite is different from the ratio obtained by the second-order perturbation theory or the three-level rotating-wave approximation. Discussion is given for the validity of this theory.

PACS numbers: 32.60.+i, 32.70.Jz, 52.70.Kz

I. INTRODUCTION

The transitions between the bound states of an atomic species in the collisionless plasma are mainly produced by absorbing or emitting an optical photon of the radiation field or the multiple microwave photons of the turbulent electric fields.

If the radiation field is composed of only the background radiation field which covers a wide spread of frequencies and polarizations, all upper levels of the allowed transitions are resonantly pumped by the background radiation field. Accordingly, the probability for finding the atom in the upper level of the allowed transition is greater than those in the upper levels of the forbidden transitions. Hence, the probability for finding the atom in the upper level of the forbidden transition is strongly dependent on those in the upper levels of the allowed transitions which are coupled with the former level by turbulent electric fields according to the electric dipole selection rules. In this case, the turbulent electric fields produce primarily Stark shifts of the allowed lines but do not significantly shift those of the forbidden lines ("asymmetrical Stark repulsion").

Theoretical treatments of the high-frequency Stark effect, based on second-order time-dependent perturbation theory, have been given by Baranger and Mozer,[1] Reinheimer,[2] and Copper and Ringler.[3] Kunze *et al.*[4] extended the perturbation calculation up to fourth order. However, these theories did not include Stark shifts of the levels. Recognizing this, Hicks *et al.*[5] have developed a theory which can include Stark shifts (actually profile). Their theory is based on two consecutive perturbation calculations, the first calculation being for the electric field and the second calculation being for the zero radiation field (spontaneous emission). They have neglected the fact that at least one intermediate upper state is not only coupled with the initial upper state by the interaction with the electric field but also with the final lower state by the induced absorption or the induced and spontaneous emission of a photon. Therefore, their theory is, in principle, valid only in the absence of the strong radiation field. Furthermore, they assumed that the upper states have equal populations, a fact that is certainly not in general true.

Recently, Prosnitz *et al.*[6] proposed a (nonperturbation) theory which explains rather well the line shape of both the satellite and allowed line in the presence of laser radiation. Their theory is based on the coupled equations for the probability amplitudes with phenomenological damping terms, but they do not include any term for the optical excitation or the radiation field. In their theory, the spectrum of the satellite lines would be the same whether the laser radiation is present or not. Hence, it is obvious that their theory cannot explain most characteristic effects caused by the radiation field. In particular, their theory will give rise to invalid results for the spectral positions and intensities of the satellite lines in the absence of the laser field. Even in the presence of the laser radiation, the satisfactory agreement between experiment[6] and theory[6] appears, in part, to be due to the use of adjustable phenomenological parameters.

For these reasons, I recently have developed a comprehensive theory which is valid for strong electric fields and includes Stark shifts of the levels for a three-level atom with two closely spaced upper levels, both in the absence and in the presence of the laser radiation.[7]

The formula for a spectral shift of the allowed line in this theory is not obtained in the theories mentioned above. Further, this theory explains the the experimental observation that the ratio of the intensity of the near satellite to that of the far satellite in the absence of a laser beam is different from the one predicted by the second-order perturbation theory,[8] or the three-level rotating-wave approximation,[6] and that the Stark repulsion is asymmetrical.

[a]Supported in part by the U.S. Office of Naval Research.

 Copyright © 1977 American Institute of Physics

This paper is an extension of the previous theory[7] to include more than two upper levels and the interaction of a magnetic field with the excited atom. I applied the theory to the σ_+, σ_-, and π components of the allowed $1\,^1S_0$-$3\,^1P_1$ line and the forbidden $1\,^1S_0$-$3\,^1D_2$ lines of the magnetic He I plasma in the absence of laser radiation. For mathematical convenience, I treat the absorption spectrum rather than the emission spectrum. The emission spectrum can be obtained similarly by taking the upper state as the initial state. Generally, both spectral profiles are not the same since the collisionless turbulent plasma is not in local thermodynamic equilibrium.[9]

II. THEORY

The time-dependent Schrödinger equation for the helium atom and the radiation field with the Coulomb potential $V(r)$ and the scalar and vector potentials Φ and $\mathbf{A}$ is

$$i\hbar\frac{\partial|\psi(t)\rangle}{\partial t}=\left(\frac{1}{2m}(\mathbf{p}-e\mathbf{A})^2+e\Phi+V(r)+\frac{e\hbar}{m}(\nabla\times\mathbf{A})\cdot\mathbf{S}+H_r\right)\times|\psi(t)\rangle, \tag{1}$$

where H_r is the quantized free radiation field Hamiltonian and S is the spin angular momentum operator.

Here, the single-particle (one-electron) state is used for describing the atomic state since, in most optical-field-producing and turbulent-field-producing transitions, the initial and final states differ only in the motion of one electron. Further, the central field approximation[10] is used for the electrostatic interactions between two electrons and the spin-orbit interaction is neglected (Russell-Saunders state).

In Eq. (1), the scalar and vector potential can be decomposed in the form

$$\mathbf{A}=\mathbf{A}^R+\mathbf{A}^M+\mathbf{A}^S\quad(\mathbf{A}^S=0), \tag{2}$$

$$\Phi=\Phi^R+\Phi^M+\Phi^S\quad(\Phi^R=\Phi^M=0), \tag{3}$$

where superscripts R, M, and S denote the radiation, static magnetic, and stochastic electric fields, respectively.

Since the stochastic field $\mathbf{E}^S$ is homogeneous within atomic dimensions, its potential $\Phi^S=\Phi$ can be written

$$\Phi(t)=-\mathbf{r}\cdot\mathbf{E}(t), \tag{4}$$

where

$$E_j(t)=\sum_k E_j^0\cos(\Omega t+\phi_j)\quad(j=x,y,z) \tag{5}$$

are the vector components of the stochastic field, E_j^0 are its amplitudes, Ω are its frequencies, and ϕ_j are its random phases. For convenience, we omit the summation notation in Eq. (5).

The vector potential $\mathbf{A}^M$ for a uniform magnetic field of induction $\mathbf{B}$ is

$$\mathbf{A}^M=\tfrac{1}{2}\mathbf{B}\times\mathbf{r}, \tag{6}$$

$$\nabla\cdot\mathbf{A}^M=0, \tag{7}$$

$$(ie\hbar/m)\mathbf{A}^M\cdot\nabla=-(e/2m)\mathbf{B}\cdot\mathbf{L}, \tag{8}$$

where $\mathbf{L}=-i\hbar\mathbf{r}\times\nabla$ is the angular momentum operator.

The perturbing radiation field is only the background field. The background field covers a wide spread of frequencies and polarizations with no phase relations between the different frequency components and polarizations. Since it is inconvenient to use the summation notations for different frequencies and polarizations everytime we write the radiation field, we will choose a typical monochromatic and linearly polarized field to calculate the probability of a transition between stationary states and omit the summation notation [therefore, we should bear in mind that $\mathbf{A}(\mathbf{r})$ is the summation of such fields]. The vector potential $\mathbf{A}$ in the Schrödinger picture for the monochromatic and linearly polarized wave field is[11]

$$\mathbf{A}(\mathbf{r})=(\hbar/2\epsilon_0\tau\omega)^{1/2}\hat{e}[a\exp(i\mathbf{k}\cdot\mathbf{r})+a^*\exp(-i\mathbf{k}\cdot\mathbf{r})], \tag{9}$$

where ϵ_0 is the dielectric constant, a and a^* are annihilation and creation operators, respectively, τ is the system volume, ω is the frequency of the wave mode, $\hat{e}$ is the photon polarization vector, and $\mathbf{k}$ is the propagation vector.

The term H_r in Eq. (1) is the energy of the quantized source-free radiation field in the absence of the atom,

$$H_r=\hbar\omega(a^*a+\tfrac{1}{2}). \tag{10}$$

The energy eigenstates of the radiation oscillator of polarization direction $\hat{e}$, momentum $\hbar\mathbf{k}$, and energy $\hbar\omega$ satisfy the eigenvalue equation

$$\hbar\omega a^*a|N\rangle=\hbar\omega N|N\rangle, \tag{11}$$

where N is the occupation number.

The numerical value of the quadratic term $(e\mathbf{A}^2/2m)$ is negligibly small even in more than the second-order perturbation calculation. Hence, we neglect it in the following. Then, by choosing the Z direction the same as the B direction, the Hamiltonian in Eq. (1) is written

$$H=H_0+H', \tag{12}$$

$$H_0=-(\hbar^2/2m)\nabla^2+V(r)-(e/2m)B_z\cdot(L_z+2S_z)+H_r \tag{13}$$

$$H'=-(e/m)(\hbar/2\epsilon_0\tau\omega)^{1/2}[a\exp(i\mathbf{k}\cdot\mathbf{r})+a^*\exp(-i\mathbf{k}\cdot\mathbf{r})]\times(\hat{e}\cdot\mathbf{p})-e\mathbf{r}\cdot\mathbf{E}(t). \tag{14}$$

An unperturbed eigenstate of H_0 may be written

$$|a,N\rangle=|a\rangle\,|N\rangle \tag{15}$$

with eigenvalue

$$E_{|a,N\rangle}=E_{|a\rangle}+N\hbar\omega, \tag{16}$$

where a refers to the atom.

Let the wave function $|\psi(t)\rangle$ of the perturbed wave equation [Eq. (1)] be expanded in terms of this complete orthonormal set $\{|a,N\rangle\}$ by

$$|\psi(t)\rangle=\sum_{|a,N\rangle}C_{|a,N\rangle}(t)\exp(-\hbar^{-1}E_{|a,N\rangle}t)\,|a,N\rangle. \tag{17}$$

By means of the orthogonality property of $|a,N\rangle$, one obtains the differential equation for the expansion coef-

ficients (probability amplitudes),

$$\frac{dC_{|a,N\rangle}(t)}{dt}=\frac{1}{i\hbar}\sum_{|a',N'\rangle}\langle a,N|H'|a',N'\rangle C_{|a',N'\rangle}(t)\times\exp(i\omega_{|a,N\rangle,|a',N'\rangle}t), \tag{18}$$

where

$$\omega_{|a,N\rangle,|a',N'\rangle}=\hbar^{-1}(E_{|a,N\rangle}-E_{|a',N'\rangle})=\hbar^{-1}(E_{|a\rangle}-E_{|a'\rangle})+(N-N')\omega. \tag{19}$$

If we use the definition of creation and annihilation operators and the orthogonality relations, we obtain by taking only the electric dipole term in expansion of $\exp(i\mathbf{k}\cdot\mathbf{r})$

$$\langle a,N|H'|a',N'\rangle=-ie\omega_{|a\rangle,|a'\rangle}(\hbar/2\epsilon_0\tau\omega)^{1/2}(\hat{e}\cdot\langle a|\mathbf{r}|a'\rangle)\times[(N'+1)^{1/2}\delta_{N,N'+1}+(N')^{1/2}\delta_{N,N'-1}]-e\mathbf{E}\cdot\langle a|\mathbf{r}|a'\rangle\delta_{N,N'}, \tag{20}$$

where

$$\omega_{|a\rangle,|a'\rangle}=\hbar^{-1}(E_{|a\rangle}-E_{|a'\rangle}). \tag{21}$$

Since $\langle a,N|H'|a',N'\rangle$ does not involve the spins and the spin functions for different S's are orthogonal, the spin state does not change in the transition. Accordingly, it will not be specified in the following.

By H_0 in Eq. (13), the unperturbed singlet atom state in the static magnetic field is specified by quantum numbers n, J, and M ($L=J$ for the singlet state), and its energy is

$$E_{|n,J,M\rangle}=E^0_{|n,J\rangle}+M\hbar\omega_L, \tag{22}$$

where ω_L is the Larmor frequency and $E^0_{|n,J\rangle}$ is the energy of the level $|n,J\rangle$ when no magnetic field is applied to the plasma. Here the intensity of the static magnetic field B is limited to the range

$$B<B_c, \tag{23}$$

where B_c is a critical value above which the Paschen-Back effect becomes important.

The selection rules of the singlet helium states are, because of $J=L$ and Eq. (20),

$$M'=M,\quad M\pm1, \tag{24}$$

$$J'=J\pm1 \tag{25}$$

for the transitions both by the radiation field and by three-dimensional stochastic fields.

In this paper, the transitions from the $n=1$ level to the $n=3$ level of the singlet helium are of interest. The atomic state $|1,0,0\rangle$ is negligibly affected by the electric fields, but the $n=3$, $J=1,2$ states are considerably affected by these fields.

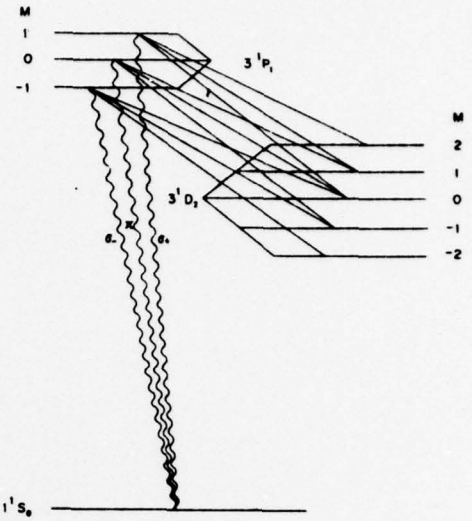

FIG. 1. Schematic diagram for transition. Wavy line: transition produced by the radiation field. Straight solid line: transition produced by the stochastic electric field.

For convenience, the states in the $n=1$ and $n=3$ level $|1,0,0\rangle$, $|3,1,1\rangle$, $|3,1,0\rangle$, $|3,1,-1\rangle$, $|3,2,2\rangle$, $|3,2,1\rangle$, $|3,2,0\rangle$, $|3,2,-1\rangle$, and $|3,2,-2\rangle$ are denoted by $0,1,\ldots,8$, respectively.

If the atom and radiation field are initially in the $|0,N_0\rangle$ states, the probability amplitude $C_i(t)=C_{|i,N_0-1\rangle}(t)$, $i=1,\ldots,8$ for finding the helium atom in the i substate of level $n=3$ after absorbing a photon of energy $\hbar\omega$ at time t is ($C_0=C_{|0,N_0\rangle}$)

$$\frac{dC_i(t)}{dt}=\frac{1}{i\hbar}\left(\sum_{j=0}\langle i|H'|j\rangle\exp(i\omega_{i,j}t)C_j(t)+\sum'_{|a,N\rangle}\langle i|H'|a,N\rangle\exp(i\omega_{i,|a,N\rangle}t)C_{|a,N\rangle}(t)\right),$$

where $|a,N\rangle$ is now the abbreviation for $|n,J,M,N\rangle$, and $\sum'_{|a,N\rangle}$ is the summation for all $|a,N\rangle$ except $i=0,\ldots,8$.

Neglecting far-off resonant terms which are small by orders of magnitude compared to the nearly or exactly resonant terms as well as the terms associated with the high-order optical transitions ($n>8$), and using the selection rules described by Eqs. (24) and (25), one can reduce Eq. (26) to[12,13]

$$\begin{aligned}\frac{dC_1(t)}{dt}&=P_1\exp[i(\omega_0+\omega_L-\omega)t]C_0(t)+C_1^4\{[E_x^0\exp(i\phi_x)+iE_y^0\exp(i\phi_y)]\exp[i(\omega_1-\omega_L+\Omega)t]\\&+[E_x^0\exp(-i\phi_x)+iE_y^0\exp(-i\phi_y)]\exp[i(\omega_1-\omega_L-\Omega)t]\}C_4(t)+C_1^4E_z^0\{\exp(i\phi_z)\exp[i(\omega_1+\Omega)t]\\&+\exp(-i\phi_z)\exp[i(\omega_1-\Omega)t]\}C_5(t)+C_1^4\{[E_x^0\exp(i\phi_x)-iE_y^0\exp(i\phi_y)]\exp[i(\omega_1+\omega_L+\Omega)t]\\&+[E_x^0\exp(-i\phi_x)-iE_y^0\exp(-i\phi_y)]\exp[i(\omega_1+\omega_L-\Omega)t]\}C_6(t),\end{aligned} \tag{27}$$

$$\begin{aligned}\frac{dC_2(t)}{dt}&=P_2\exp[i(\omega_0-\omega)t]C_0(t)+C_2^4\{[E_x^0\exp(i\phi_x)+iE_y^0\exp(i\phi_y)]\exp[i(\omega_1-\omega_L+\Omega)t]\\&+[E_x^0\exp(-i\phi_x)+iE_y^0\exp(-i\phi_y)]\exp[i(\omega_1-\omega_L-\Omega)t]\}C_5(t)+C_2^4E_z^0\{\exp(i\phi_z)\exp[i(\omega_1+\Omega)t]\end{aligned}$$

$$+\exp(-i\phi_z)\exp[i(\omega_1-\Omega)t]\}C_6(t)+C_2^7\{[E_x^0\exp(i\phi_x)-iE_y^0\exp(i\phi_y)]\exp[i(\omega_1+\omega_L+\Omega)t]$$
$$+[E_x^0\exp(-i\phi_x)-iE_y^0\exp(-i\phi_y)]\exp[i(\omega_1+\omega_L-\Omega)t]\}C_7(t), \tag{28}$$

$$\frac{dC_3(t)}{dt}=P_3\exp[i(\omega_0-\omega_L-\omega)t]C_0(t)+C_3^6\{[E_x^0\exp(i\phi_x)+iE_y^0\exp(i\phi_y)]\exp[i(\omega_1-\omega_L+\Omega)t]$$
$$+[E_x^0\exp(-i\phi_x)+iE_y^0\exp(-i\phi_y)]\exp[i(\omega_1-\omega_L-\Omega)t]\}C_6(t)+C_3^7E_z^0\{\exp(i\phi_z)\exp[i(\omega_1+\Omega)t]$$
$$+\exp(-i\phi_z)\exp[i(\omega_1-\Omega)t]\}C_7(t)+C_3^8\{[E_x^0\exp(i\phi_x)-iE_y^0\exp(i\phi_y)]\exp[i(\omega_1+\omega_L+\Omega)t]$$
$$+[E_x^0\exp(-i\phi_x)-iE_y^0\exp(-i\phi_y)]\exp[i(\omega_1+\omega_L-\Omega)t]\}C_8(t), \tag{29}$$

$$\frac{dC_4(t)}{dt}=-C_1^4{}^*\{[E_x^0\exp(i\phi_x)-iE_y^0\exp(i\phi_y)]\exp[i(-\omega_1+\omega_L+\Omega)t]+[E_x^0\exp(-i\phi_x)-iE_y^0\exp(-i\phi_y)]$$
$$\times\exp[i(-\omega_1+\omega_L-\Omega)t]\}C_1(t), \tag{30}$$

$$\frac{dC_5(t)}{dt}=-C_1^5{}^*E_z^0\{\exp(i\phi_z)\exp[i(-\omega_1+\Omega)t]+\exp(-i\phi_z)\exp[i(-\omega_1-\Omega)t]\}C_1(t)$$
$$-C_2^5{}^*\{[E_x^0\exp(i\phi_x)-iE_y^0\exp(i\phi_y)]\exp[i(-\omega_1+\omega_L+\Omega)t]+[E_x^0\exp(-i\phi_x)-iE_y^0\exp(-i\phi_y)]$$
$$\times\exp[i(-\omega_1+\omega_L-\Omega)t]\}C_2(t), \tag{31}$$

$$\frac{dC_6(t)}{dt}=-C_1^6{}^*\{[E_x^0\exp(i\phi_x)+iE_y^0\exp(i\phi_y)]\exp[i(-\omega_1-\omega_L+\Omega)t]+[E_x^0\exp(-i\phi_x)+iE_y^0\exp(-i\phi_y)]$$
$$\times\exp[i(-\omega_1-\omega_L-\Omega)t]\}C_1(t)-C_2^6{}^*E_z^0\{\exp(i\phi_z)\exp[i(-\omega_1+\Omega)t]+\exp(-i\phi_z)\exp[i(-\omega_1-\Omega)t]\}C_2(t)$$
$$-C_3^6{}^*\{[E_x^0\exp(i\phi_x)-iE_y^0\exp(i\phi_y)]\exp[i(-\omega_1+\omega_L+\Omega)t]+[E_x^0\exp(-i\phi_x)-iE_y^0\exp(-i\phi_y)]$$
$$\times\exp[i(-\omega_1+\omega_L-\Omega)t]\}C_3(t), \tag{32}$$

$$\frac{dC_7(t)}{dt}=-C_2^7{}^*\{[E_x^0\exp(i\phi_x)+iE_y^0\exp(i\phi_y)]\exp[i(-\omega_1-\omega_L+\Omega)t]+[E_x^0\exp(-i\phi_x)+iE_y^0\exp(-i\phi_y)]$$
$$\times\exp[i(-\omega_1-\omega_L-\Omega)t]\}C_2(t)-C_3^7{}^*E_z^0\{\exp(i\phi_z)\exp[i(-\omega_1+\Omega)t]+\exp(-i\phi_z)\exp[i(-\omega_1-\Omega)t]\}C_3(t), \tag{33}$$

$$\frac{dC_8(t)}{dt}=-C_3^8{}^*\{[E_x^0\exp(i\phi_x)+iE_y^0\exp(i\phi_y)]\exp[i(-\omega_1-\omega_L+\Omega)t]$$
$$+[E_x^0\exp(-i\phi_x)+iE_y^0\exp(-i\phi_y)]\exp[i(-\omega_1-\omega_L-\Omega)t]\}C_3(t), \tag{34}$$

where

$$P_1=-\tfrac{1}{2}e(\omega_0+\omega_L)(e_x-ie_y)\langle 1|x+iy|0\rangle(N/2\epsilon_0\tau\hbar\omega)^{1/2}, \tag{35}$$
$$P_2=-e\omega_0e_z\langle 2|z|0\rangle(N/2\epsilon_0\tau\hbar\omega)^{1/2}, \tag{36}$$
$$P_3=-\tfrac{1}{2}e(\omega_0-\omega_L)(e_x+ie_y)\langle 3|x-iy|0\rangle(N/2\epsilon_0\tau\hbar\omega)^{1/2}, \tag{37}$$
$$C_1^4=(ie/4\hbar)\langle 1|x-iy|4\rangle,\quad C_1^5=(ie/2\hbar)\langle 1|z|5\rangle,\quad C_1^6=(ie/4\hbar)\langle 1|x+iy|6\rangle, \tag{38}$$
$$C_2^5=(ie/4\hbar)\langle 2|x-iy|5\rangle,\quad C_2^6=(ie/2\hbar)\langle 2|z|6\rangle,\quad C_2^7=(ie/4\hbar)\langle 2|x+iy|7\rangle, \tag{39}$$
$$C_3^6=(ie/4\hbar)\langle 3|x-iy|6\rangle,\quad C_3^7=(ie/2\hbar)\langle 3|z|7\rangle,\quad C_3^8=(ie/4\hbar)\langle 3|x+iy|8\rangle. \tag{40}$$

In these equations, e_j represents the j component of the polarization vector, C_i^{j*} denotes the complex conjugate of C_i^j, $\omega_0=\omega_{1,0}$ and $\omega_1=\hbar^{-1}(E^0_{|3,1\rangle}-E^0_{|3,2\rangle})$. Figure 1 is a schematic diagram showing the transitions corresponding to Eqs. (27)–(34).

The $0\rightsquigarrow i$ atomic transition probabilities per unit time are given by

$$T_i=|C_i(t)|^2t^{-1}\quad(i=1,\ldots,8), \tag{41}$$

where t is much smaller than the lifetime of level 0, but much greater than $2\pi/\Omega$. Accordingly, one can write

$$C_0(t)\approx 1, \tag{42}$$
$$C_i(t)\ll 1\quad(i=1,\ldots,8). \tag{43}$$

It should be noted that even if $C_i(t)\ll 1$, $i=1,\ldots,8$, there can still be an effect of observable magnitude if a large number of independent systems contribute.

Substituting Eq. (42) into Eq. (27) and integrating by parts, one obtains

$$C_1(t)=P_1\frac{\exp[i(\omega_0+\omega_L-\omega)t]-1}{i(\omega_0+\omega_L-\omega)}+C_1^4\Bigg([E_x^0\exp(i\phi_x)+iE_y^0\exp(i\phi_y)]\frac{\exp[i(\omega_1-\omega_L+\Omega)t]}{i(\omega_1-\omega_L+\Omega)}$$
$$+[E_x^0\exp(-i\phi_x)+iE_y^0\exp(-i\phi_y)]\frac{\exp[i(\omega_1-\omega_L-\Omega)t]}{i(\omega_1-\omega_L-\Omega)}\Bigg)C_4(t)+C_1^5E_z^0\Bigg(\exp(i\phi_z)\frac{\exp[i(\omega_1+\Omega)t]}{i(\omega_1+\Omega)}$$

$$+\exp(-i\phi_z)\frac{\exp[i(\omega_1-\Omega)t]}{i(\omega_1-\Omega)}\Big)C_5(t)+C_1^0\Big([E_x^0\exp(i\phi_x)-iE_y^0\exp(i\phi_y)]\frac{\exp[i(\omega_1+\omega_L+\Omega)t]}{i(\omega_1+\omega_L+\Omega)}$$

$$+[E_x^0\exp(-i\phi_x)-iE_y^0\exp(-i\phi_y)]\frac{\exp[i(\omega_1+\omega_L-\Omega)t]}{i(\omega_1+\omega_L-\Omega)}\Big)C_6(t)-\int_0^t\Big[C_1^0\Big([E_x^0\exp(i\phi_x)+iE_y^0\exp(i\phi_y)]$$

$$\times\frac{\exp[i(\omega_1-\omega_L+\Omega)t]}{i(\omega_1-\omega_L+\Omega)}+[E_x^0\exp(-i\phi_x)+iE_y^0\exp(-i\phi_y)]\frac{\exp[i(\omega_1-\omega_L-\Omega)t]}{i(\omega_1-\omega_L-\Omega)}\Big)\frac{dC_4(t)}{dt}+C_1^0E_z^0$$

$$\times\Big(\exp(i\phi_z)\frac{\exp[i(\omega_1+\Omega)t]}{i(\omega_1+\Omega)}+\exp(-i\phi_z)\frac{\exp[i(\omega_1-\Omega)t]}{i(\omega_1-\Omega)}\Big)\frac{dC_5(t)}{dt}+C_1^0\Big([E_x^0\exp(i\phi_x)-iE_y^0\exp(i\phi_y)]\frac{\exp[i(\omega_1+\omega_L+\Omega)t]}{i(\omega_1+\omega_L+\Omega)}$$

$$+[E_x^0\exp(-i\phi_x)-iE_y^0\exp(-i\phi_y)]\frac{\exp[i(\omega_1+\omega_L-\Omega)t]}{i(\omega_1+\omega_L-\Omega)}\Big)\frac{dC_6(t)}{dt}\Big]dt. \tag{44}$$

Because of the assumption on the transition probability as described in Eq. (43), the second, third, and fourth terms at the right-hand side of the above equation are neglected in comparison to the rest. This is also justifiable by the direct estimation of these terms as will be seen in Sec. IV.

In view of Eqs. (30)–(32), $dC_4(t)/dt$, $dC_5(t)/dt$, and $dC_6(t)/dt$ cannot be neglected.

Substituting Eqs. (30)–(32) into Eq. (44) and differentiating with respect to t yields

$$\frac{dC_1(t)}{dt}-f_1(t)C_1(t)=g_1(t), \tag{45}$$

which has the solution

$$C_1(t)=\exp\Big[\int_0^t f(t')\,dt'\Big]\int_0^t g_1(t')\exp\Big[\int_0^{t'}f(t'')\,dt''\Big]dt', \tag{46}$$

where

$$f_1(t)=|C_1^0|^2\Big([E_x^0\exp(i\phi_x)+iE_y^0\exp(i\phi_y)][E_x^0\exp(i\phi_x)-iE_y^0\exp(i\phi_y)]\frac{\exp(i2\Omega t)}{i(\omega_1-\omega_L+\Omega)}+|E_x^0\exp(-i\phi_x)+iE_y^0\exp(-i\phi_y)|^2$$

$$\times[i(\omega_1-\omega_L-\Omega)]^{-1}+|E_x^0\exp(i\phi_x)+iE_y^0\exp(i\phi_y)|^2[i(\omega_1-\omega_L+\Omega)]^{-1}+[E_x^0\exp(-i\phi_x)+iE_y^0\exp(-i\phi_y)]$$

$$\times[E_x^0\exp(-i\phi_x)-iE_y^0\exp(-i\phi_y)]\frac{\exp(-i2\Omega t)}{i(\omega_1-\omega_L-\Omega)}\Big)+|C_1^0|^2E_z^{0^2}\Big(\exp(i2\phi_z)\frac{\exp(i2\Omega t)}{i(\omega_1+\Omega)}+\frac{1}{i(\omega_1-\Omega)}+\frac{1}{i(\omega_1+\Omega)}$$

$$+\exp(-i2\phi_z)\frac{\exp(-i2\Omega t)}{i(\omega_1-\Omega)}\Big)+|C_1^0|^2\Big([E_x^0\exp(i\phi_x)-iE_y^0\exp(i\phi_y)][E_x^0\exp(i\phi_x)+iE_y^0\exp(i\phi_y)]\frac{\exp(i2\Omega t)}{i(\omega_1+\omega_L+\Omega)}$$

$$+|E_x^0\exp(-i\phi_x)-iE_y^0\exp(-i\phi_y)|^2[i(\omega_1+\omega_L-\Omega)]^{-1}+|E_x^0\exp(i\phi_x)-iE_y^0\exp(i\phi_y)|^2[i(\omega_1+\omega_L+\Omega)]^{-1}$$

$$+[E_x^0\exp(-i\phi_x)-iE_y^0\exp(-i\phi_y)][E_x^0\exp(-i\phi_x)+iE_y^0\exp(-i\phi_y)]\frac{\exp(-i2\Omega t)}{i(\omega_1+\omega_L-\Omega)}\Big) \tag{47}$$

and

$$g_1(t)=P_1\exp[i(\omega_0+\omega_L-\omega)t]+\Big[C_1^0C_2^{0*}E_z^0\Big(\exp(i\phi_z)\frac{\exp[i(\omega_1+\Omega)t]}{i(\omega_1+\Omega)}+\exp(-i\phi_z)\frac{\exp[i(\omega_1-\Omega)t]}{i(\omega_1-\Omega)}\Big)$$

$$\times\{[E_x^0\exp(i\phi_x)-iE_y^0\exp(i\phi_y)]\exp[i(-\omega_1+\omega_L+\Omega)t]+[E_x^0\exp(-i\phi_x)-iE_y^0\exp(-i\phi_y)]\exp[i(-\omega_1+\omega_L-\Omega)t]\}$$

$$+C_1^0C_2^{0*}E_z^0\Big([E_x^0\exp(i\phi_x)-iE_y^0\exp(i\phi_y)]\frac{\exp[i(\omega_1+\omega_L+\Omega)t]}{i(\omega_1+\omega_L+\Omega)}+[E_x^0\exp(-i\phi_x)-iE_y^0\exp(-i\phi_y)]\frac{\exp[i(\omega_1+\omega_L-\Omega)t]}{i(\omega_1+\omega_L-\Omega)}\Big)$$

$$\times\{\exp(i\phi_z)\exp[i(-\omega_1+\Omega)t]+\exp(-i\phi_z)\exp[i(-\omega_1-\Omega)t]\}\Big]C_2(t)+C_1^0C_2^{0*}\Big([E_x^0\exp(i\phi_x)-iE_y^0\exp(i\phi_y)]$$

$$\times\frac{\exp[i(\omega_1+\omega_L+\Omega)t}{i(\omega_1+\omega_L+\Omega)}+[E_x^0\exp(-i\phi_x)-iE_y^0\exp(-i\phi_y)]\frac{\exp[i(\omega_1+\omega_L-\Omega)t]}{i(\omega_1+\omega_L-\Omega)}\Big)$$

$$\times\{[E_x^0\exp(i\phi_x)-iE_y^0\exp(i\phi_y)]\exp[i(-\omega_1+\omega_L+\Omega)t]+[E_x^0\exp(-i\phi_x)-iE_y^0\exp(-i\phi_y)]\exp[i(-\omega_1+\omega_L-\Omega)t]\}C_3(t). \tag{48}$$

Because of the random properties of phase, the direction, and the amplitude, and the high frequency ($\Omega t\gg 1$) of the stochastic electric fields, $\int_0^t f_1(t')\,dt'$ fluctuates negligibly about

$$\Big\langle\int_0^t f_1(t')\,dt'\Big\rangle=-i\Delta\omega_1 t, \tag{49}$$

where

$$\Delta\omega_1=\frac{e^2\langle E^2\rangle}{3\hbar^2}\Big(\frac{|\langle 1|x-iy|4\rangle|^2(\omega_1-\omega_L)}{2[(\omega_1-\omega_L)^2-\Omega^2]}+\frac{|\langle 1|z|5\rangle|^2\omega_1}{\omega_1^2-\Omega^2}+\frac{|\langle 1|x+iy|6\rangle|^2(\omega_1+\omega_L)}{2[(\omega_1+\omega_L)^2-\Omega^2]}\Big)$$

$$= \frac{Qe^2\langle E^2\rangle a_0^2}{3\hbar^2}\left(\frac{6(\omega_1-\omega_L)}{(\omega_1-\omega_L)^2-\Omega^2}+\frac{3\omega_1}{\omega_1^2-\Omega^2}+\frac{\omega_1+\omega_L}{(\omega_1+\omega_L)^2-\Omega^2}\right). \tag{50}$$

In these equations, $\langle\,\rangle$ means the average over the phase, the direction, and the amplitude of the stochastic fields, a_0 denotes the Bohr radius, $Q=6.7$, and ω_1 is 104 cm^{-1} in wave-number units.

Accordingly, one obtains

$$C_1(t)=\exp(-i\Delta\omega_1 t)\int_0^t g_1(t')\exp(i\Delta\omega_1 t')\,dt' \approx P_1\exp(-i\Delta\omega_1 t)\int_0^t \exp[i(\omega_0+\omega_L+\Delta\omega_1-\omega)t']\,dt' \tag{51}$$

and

$$T_1 = 2\pi|P_1|^2\delta(\omega_0+\omega_L+\Delta\omega_1-\omega). \tag{52}$$

In these equations, the second and third terms of Eq. (48) are neglected compared to the first term. It will be justified in Sec. IV.

Equation (52) means that the $0\rightarrow 1$ allowed line (σ_+ line) is shifted as much as $\Delta\omega_1$, which is proportional to the mean-square stochastic electric field (the quadratic Stark effect). Similarly, the probability amplitudes and the transition probabilities for the 2 and 3 levels (π and σ_- lines) are

$$C_2(t)=P_2\exp(-i\Delta\omega_2 t)\int_0^t \exp[i(\omega_0+\Delta\omega_2-\omega)t']\,dt', \tag{53}$$

$$T_2 = 2\pi|P_2|^2\delta(\omega_0+\Delta\omega_2-\omega), \tag{54}$$

where

$$\Delta\omega_2 = \frac{e^2\langle E^2\rangle}{3\hbar^2}\left(\frac{|\langle 2|x-iy|5\rangle|^2(\omega_1-\omega_L)}{2[(\omega_1-\omega_L)^2-\Omega^2]}+\frac{|\langle 2|z|6\rangle|^2\omega_1}{\omega_1^2-\Omega^2}+\frac{|\langle 2|x+iy|7\rangle|^2(\omega_1+\omega_L)}{2[(\omega_1+\omega_L)^2-\Omega^2]}\right)$$

$$= \frac{Qe^2\langle E^2\rangle a_0^2}{3\hbar^2}\left(\frac{3(\omega_1-\omega_L)}{(\omega_1-\omega_L)^2-\Omega^2}+\frac{4\omega_1}{\omega_1^2-\Omega^2}+\frac{3(\omega_1+\omega_L)}{(\omega_1+\omega_L)^2-\Omega^2}\right), \tag{55}$$

$$C_3(t)=P_3\exp(-i\Delta\omega_3 t)\int_0^t \exp[i(\omega_0-\omega_L+\Delta\omega_3-\omega)t']\,dt', \tag{56}$$

$$T_3 = 2\pi|P_3|^2\delta(\omega_0-\omega_L+\Delta\omega_3-\omega), \tag{57}$$

where

$$\Delta\omega_3 = \frac{e^2\langle E^2\rangle}{3\hbar^2}\left(\frac{|\langle 3|x-iy|6\rangle|^2(\omega_1-\omega_L)}{2[(\omega_1-\omega_L)^2-\Omega^2]}+\frac{|\langle 3|z|7\rangle|^2\omega_1}{\omega_1^2-\Omega^2}+\frac{|\langle 3|x+iy|8\rangle|^2(\omega_1+\omega_L)}{2(\omega_1+\omega_L)^2-\Omega^2}\right)$$

$$= \frac{Qe^2\langle E^2\rangle a_0^2}{3\hbar^2}\left(\frac{\omega_1-\omega_L}{(\omega_1-\omega_L)^2-\Omega^2}+\frac{3\omega_1}{\omega_1^2-\Omega^2}+\frac{6(\omega_1+\omega_L)}{(\omega_1+\omega_L)^2-\Omega^2}\right). \tag{58}$$

Substitution of Eq. (51) into Eq. (30) yields

$$C_4(t)=\frac{P_1C_1^*}{(\omega_0+\omega_L+\Delta\omega_1-\omega)}\left[[E_x^0\exp(i\phi_x)-iE_y^0\exp(i\phi_y)]\left(\frac{\exp[i(\omega_0-\omega_1+2\omega_L+\Omega-\omega)t]-1}{\omega_0-\omega_1+2\omega_L+\Omega-\omega}\right.\right.$$
$$\left.+\frac{\exp[i(-\omega_1+\omega_L-\Delta\omega_1+\Omega)t]-1}{-\omega_1+\omega_L-\Delta\omega_1+\Omega}\right)+[E_x^0\exp(-i\phi_x)-iE_y^0\exp(-i\phi_y)]$$
$$\left.\times\left(\frac{\exp[i(\omega_0-\omega_1+2\omega_L-\Omega-\omega)t]-1}{\omega_0-\omega_1+2\omega_L-\Omega-\omega}+\frac{\exp[i(-\omega_1+\omega_L-\Delta\omega_1-\Omega)t]-1}{-\omega_1+\omega_L-\Delta\omega_1-\Omega}\right)\right]. \tag{59}$$

Accordingly, the probability for the transition $0\rightarrow 4$ is

$$T_4=\frac{2\pi|P_1|^2e^2|\langle 1|x-iy|4\rangle|^2\langle E^2\rangle}{12\hbar^2(\omega_0+\omega_L+\Delta\omega_1-\omega)^2}[\delta(\omega_0-\omega_1+2\omega_L+\Omega-\omega)+\delta(\omega_0-\omega_1+2\omega_L-\Omega-\omega)] \quad (-\omega_1+\omega_L-\Delta\omega_1\pm\Omega\neq 0). \tag{60}$$

Similarly one obtains for the probabilities for the transitions $0\rightarrow 5$, $0\rightarrow 6$, $0\rightarrow 7$, $0\rightarrow 8$ as

$$T_5=\frac{2\pi e^2\langle E^2\rangle}{6\hbar^2}\left(\frac{|P_1|^2|\langle 1|z|5\rangle|^2}{(\omega_0+\omega_L+\Delta\omega_1-\omega)^2}+\frac{|P_2|^2|\langle 2|x-iy|5\rangle|^2}{2(\omega_0+\Delta\omega_2-\omega)^2}\right)[\delta(\omega_0-\omega_1+\omega_L+\Omega-\omega)+\delta(\omega_0-\omega_1+\omega_L-\Omega-\omega)], \tag{61}$$

$$T_6=\frac{2\pi e^2\langle E^2\rangle}{6\hbar^2}\left(\frac{|P_1|^2|\langle 1|x+iy|6\rangle|^2}{2(\omega_0+\omega_L+\Delta\omega_1-\omega)^2}+\frac{|P_3|^2|\langle 3|x-iy|6\rangle|^2}{2(\omega_0-\omega_L+\Delta\omega_3-\omega)^2}+\frac{|P_2|^2|\langle 2|z|6\rangle|^2}{(\omega_0+\Delta\omega_2-\omega)^2}\right)$$
$$\times[\delta(\omega_0-\omega_1+\Omega-\omega)+\delta(\omega_0-\omega_1-\Omega-\omega)], \tag{62}$$

$$T_7=\frac{2\pi e^2\langle E^2\rangle}{6\hbar^2}\left(\frac{|P_2|^2|\langle 2|x+iy|7\rangle|^2}{2(\omega_0+\Delta\omega_2-\omega)^2}+\frac{|P_3|^2|\langle 3|z|7\rangle|^2}{(\omega_0-\omega_L+\Delta\omega_3-\omega)^2}\right)[\delta(\omega_0-\omega_1-\omega_L+\Omega-\omega)+\delta(\omega_0-\omega_1-\omega_L-\Omega-\omega)], \tag{63}$$

$$T_8=\frac{2\pi|P_3|^2e^2|\langle 3|x+iy|8\rangle|^2\langle E^2\rangle}{12\hbar^2(\omega_0-\omega_L+\Delta\omega_3-\omega)^2}[\delta(\omega_0-\omega_1-2\omega_L+\Omega-\omega)+\delta(\omega_0-\omega_1-2\omega_L-\Omega-\omega)]. \tag{64}$$

In these equations, we used $|P_1|^2 = |P_2|^2 = |P_3|^2$, which comes from the fact that the radiation intensity does not change significantly in the range of $\omega_1 + 2\omega_L$ about ω_0.

In deriving Eq. (62), we neglect $P_1 P_2^*$ and $P_1^* P_2$ since the average of the cross terms between the different frequency components with no phase relations of the radiation field is zero.

Equations (60)–(64) mean that there are two satellites disposed symmetrically in pairs about each of the forbidden lines, $0 \to 4$, $0 \to 5$, $0 \to 6$, $0 \to 7$, and $0 \to 8$, and separated from them by Ω.

It is important to point out that the spectral shift of the satellite line is not seen in Eqs. (60)–(64) ("asymmetrical Stark repulsion"). The spectral shift of the satellite line can be seen in the case of the selective excitation of the forbidden transition by the laser. This result cannot be explained by the coupled equations with the phenomenological damping constants of Prosnitz *et al.*[6] Similar results have been found by Griem[14] since Griem has not treated the laser radiation.

The ratios of the absorption coefficients at these satellite frequencies to that of the allowed line are

$$S_a^4 = \frac{Qe^2 a_0^2 \langle E^2 \rangle}{\hbar^2 (\omega_1 - \omega_L + \Delta\omega_1 \pm \Omega)^2}, \tag{65}$$

$$S_a^6 = \frac{Qe^2 a_0^2 \langle E^2 \rangle}{2\hbar^2} \left(\frac{1}{(\omega_1 + \Delta\omega_1 \pm \Omega)^2} + \frac{1}{(\omega_1 - \omega_L + \Delta\omega_2 \pm \Omega)^2} \right), \tag{66}$$

$$S_a^6 = \frac{Qe^2 a_0^2 \langle E^2 \rangle}{6\hbar^2} \left(\frac{1}{(\omega_1 + \omega_L + \Delta\omega_1 \pm \Omega)^2} + \frac{1}{(\omega_1 - \omega_L + \Delta\omega_3 \pm \Omega)^2} + \frac{4}{(\omega_1 + \Delta\omega_2 \pm \Omega)^2} \right), \tag{67}$$

$$S_a^7 = \frac{Qe^2 a_0^2 \langle E^2 \rangle}{2\hbar^2} \left(\frac{1}{(\omega_1 + \omega_L + \Delta\omega_2 \pm \Omega)^2} + \frac{1}{(\omega_1 + \Delta\omega_3 \pm \Omega)^2} \right), \tag{68}$$

$$S_a^8 = \frac{Qe^2 a_0^2 \langle E^2 \rangle}{\hbar^2 (\omega_1 + \omega_L + \Delta\omega_3 \pm \Omega)^2}, \tag{69}$$

for $0 \to 4$, $0 \to 5$, $0 \to 6$, $0 \to 7$, and $0 \to 8$ satellites, respectively, where the minus sign in the above formulas corresponds to the near satellite and the plus sign to the far satellites.

If $B = 0$ ($\omega_L = 0$), there are only two satellites disposed symmetrically in pairs about a forbidden $1\,^1S_0$-$3\,^1D_2$ line and separated from it by Ω. The ratio S_a defined above in this case is

$$S_a = \frac{5Qe^2 a_0^2 \langle E^2 \rangle}{\hbar^2 (\omega_1 + \Delta\omega \pm \Omega)^2}, \tag{70}$$

where

$$\Delta\omega = \frac{10Qe^2 a_0^2 \langle E^2 \rangle}{3\hbar^2} \frac{\omega_1}{\omega_1^2 - \Omega^2}. \tag{71}$$

It should be pointed out that S_a given by Baranger and Mozer[1] as

$$S_a^{BM} = \frac{R_{1,2} c^2 a_0^2 \langle E^2 \rangle}{6\hbar^2 (\omega_1 \pm \Omega)^2} = \frac{5Qe^2 a_0^2 \langle E^2 \rangle}{3\hbar^2 (\omega_1 \pm \Omega)^2} \quad (R_{1,2} = 10Q = 67) \tag{72}$$

has a factor and a denominator which are different from Eq. (71) by $\frac{1}{3}$, and by $\Delta\omega \neq 0$, respectively.

The perturbation calculations by Baranger and Mozer[1] and Griem[15] could not include the detailed coupling mechanism between the upper states of the allowed and forbidden transitions and the Stark shifts of the allowed lines. The deficiency in the coupling mechanism gives rise to the above difference in factor and the fault that does not include the Stark shift to $\Delta\omega \neq 0$ of the denominator. The three-level rotating-wave approximation of Prosnitz *et al.*[6] has the former deficiency as the perturbation theory and would give rise to a different denominator since their theory would claim Stark shifts of the satellites in the absence of the laser radiation.

III. CONCLUSIONS

A theory of the spectral shifts of σ_+, σ_-, and π components of the allowed line ($1\,^1S_0$-$3\,^1P_1$) and the satellites about the forbidden line ($1\,^1S_0$-$3\,^1D_2$) of a He I plasma in the static magnetic field has been developed from first principles, in which the atomic states are exposed to (longitudinal) turbulent electric fields and (transverse) radiation fields. The σ_+, σ_-, and π components of the allowed line are shifted as much as $\Delta\omega_1$, $\Delta\omega_2$, and $\Delta\omega_3$, respectively, while the satellite lines are not. The ratio of the integrated intensity of the satellite line to that of the allowed line is different from the ratio obtained from the second-order perturbation theory[1] or the three-level rotating-wave approximation.[6] From the observation of the distance in frequency between two satellites of a forbidden line and of the shifts of the allowed lines or the ratio of the integrated intensity of the satellite line to that of allowed line, a quantitative determination of the frequency and intensity of the stochastic electric field is possible.

IV. VALIDITY OF THEORY

We discuss as to whether the solutions for $C_1(t)$, $C_2(t)$, and $C_3(t)$ given in Eqs. (51), (53), and (56), respectively, are good approximate solutions of the coupled equations (27)–(24). In the following, we denote $C_i(t)$, $i = 1, 2, 3$ given in Eqs. (51), (53), and (56) as $C_i^a(t)$, $i = 1, 2, 3$ in order to distinguish from the exact solutions $C_i(t)$, $i = 1, 2, 3$.

(i) First, we prove that $C_1^a(t)$ satisfies the following approximate equation:

$$\frac{dC_1^a(t)}{dt} - f_1(t) C_1^a(t) \approx g_1^a(t), \tag{73}$$

where $g_1^a(t)$ can be expressed by replacing $C_i(t)$ with $C_i^a(t)$ in Eq. (48).

Since $C_1^a(t)$ satisfies

$$\frac{dC_1^a(t)}{dt} - f_1(t) C_1^a(t) = P_1 \exp[i(\omega_0 + \omega_L - \omega)t], \tag{74}$$

the validity of Eq. (73) depends on that

$$h_1(t) = \Bigg| \int_0^t \Bigg\{ \Bigg[C_1^{\dagger} C_2^{\dagger *} E_x^0 \Bigg(\exp(i\phi_x) \frac{\exp[i(\omega_1 + \Omega)t']}{i(\omega_1 + \Omega)} + \exp(-i\phi_x) \frac{\exp[i(\omega_1 - \Omega)t']}{i(\omega_1 - \Omega)} \Bigg)$$
$$\times \{ [E_x^0 \exp(i\phi_x) - iE_y^0 \exp(i\phi_y)] \exp[i(-\omega_1 + \omega_L + \Omega)t'] + [E_x^0 \exp(-i\phi_x) - iE_y^0 \exp(-i\phi_y)] \exp[i(-\omega_1 + \omega_L - \Omega)t'] \}$$
$$+ C_1^{\dagger} C_4^{\dagger *} E_x^0 \Bigg([E_x^0 \exp(i\phi_x) - iE_y^0 \exp(i\phi_y)] \frac{\exp[i(\omega_1 + \omega_L + \Omega)t']}{i(\omega_1 + \omega_L + \Omega)} + [E_x^0 \exp(-i\phi_x) - iE_y^0 \exp(-i\phi_y)]$$
$$\times \frac{\exp[i(\omega_1 + \omega_L - \Omega)t']}{i(\omega_1 + \omega_L - \Omega)} \Bigg) \{ \exp(i\phi_x) \exp[i(-\omega_1 + \Omega)t'] + \exp(-i\phi_x) \exp[i(-\omega_1 - \Omega)t'] \} \Bigg] C_3^{\dagger}(t')$$
$$+ C_1^{\dagger} C_3^{\dagger *} \Bigg([E_x^0 \exp(i\phi_x) - iE_y^0 \exp(i\phi_y)] \frac{\exp[i(\omega_1 + \omega_L + \Omega)t']}{i(\omega_1 + \omega_L + \Omega)} + [E_x^0 \exp(-i\phi_x) - iE_y^0 \exp(-i\phi_y)]$$
$$\times \frac{\exp[i(\omega_1 + \omega_L - \Omega)t']}{i(\omega_1 + \omega_L - \Omega)} \Bigg) \{ [E_x^0 \exp(i\phi_x) - iE_y^0 \exp(i\phi_y)] \exp[i(-\omega_1 + \omega_L + \Omega)t']$$
$$+ [E_x^0 \exp(-i\phi_x) - iE_y^0 \exp(-i\phi_y)] \exp[i(-\omega_1 + \omega_L - \Omega)t'] \} C_3^{\dagger}(t') \Bigg\} \exp(i\Delta\omega_1 t')\, dt' \Bigg|^2 \tag{75}$$

can be ignored in comparison to

$$|C_1^{\dagger}(t)|^2 = \Big| \int_0^t P_1 \exp[i(\omega_0 + \omega_L + \Delta\omega_1 - \omega)t]\, dt \Big|^2 = 2\pi t |P_1|^2, \tag{76}$$

where the summation with respect to ω has been made in Eq. (76), since the radiation field covers a wide spread of frequencies and the contributions from various frequencies are additive.

From the direct calculation of Eq. (75) after substituting $C_2^{\dagger}(t)$ and $C_3^{\dagger}(t)$,

$$|C_1^{\dagger}|^2, \quad |C_2^{\dagger}|^2, \quad |C_1^{\dagger}|^2, \quad |C_3^{\dagger}|^2 \ll (Qe^2 a_0^2/\hbar^2) \tag{77}$$

and

$$\omega_L, \quad \Omega, \quad \Delta\omega_1, \quad \Delta\omega_2, \quad \Delta\omega_3 \ll \omega_1 \tag{78}$$

for most experimental cases, we can be sure that if

$$\frac{1}{(\omega_L + 2\Omega_2 + \Delta\omega_1 - \Delta\omega_2)^2}, \quad \frac{1}{(\omega_L - 2\Omega + \Delta\omega_1 - \Delta\omega_2)^2}, \quad \frac{1}{(\omega_L + \Delta\omega_1 - \Delta\omega_2)^2} \ll \frac{\hbar^4 \omega_1^2}{(Qa_0^2)^2 e^4 \langle E^2 \rangle^2} \tag{79}$$

and

$$\frac{1}{(2\omega_L + \Delta\omega_1 - \Delta\omega_3)^2}, \quad \frac{1}{(2\omega_L + 2\Omega + \Delta\omega_1 - \Delta\omega_3)^2}, \quad \frac{1}{(2\omega_L - 2\Omega + \Delta\omega_1 - \Delta\omega_3)^2} \ll \frac{\hbar^4 \omega_1^2}{(Qa_0^2)^2 e^4 \langle (E^2)^2 \rangle}, \tag{80}$$

$h_1(t)$ can be ignored in comparison with $|C_1^{\dagger}(t)|^2$. Inequalities (79) and (80) are the same as the criteria for the validity of the perturbation calculation, which can be stated in a crude form that $\hbar\omega_L$ and $|\hbar\omega_L - 2\hbar\Omega|$ are greater than the perturbing energy of the electric field E_p, where

$$E_p \sim (10Q)^{1/2} ea \langle (E^2) \rangle^{1/2}. \tag{81}$$

(ii) We proved that $C_1^{\dagger}(t)$ satisfies Eq. (73). Hence, $C_1^{\dagger}(t)$ obviously satisfies

$$C_1^{\dagger}(t) \approx P_1 \frac{\exp[i(\omega_0 + \omega_L - \omega)t] - 1}{i(\omega_0 + \omega_L - \omega)} - U(t), \tag{82}$$

where

$$U(t) = -\int_0^t \Bigg[C_1^{\dagger} \Bigg([E_x^0 \exp(i\phi_x) + iE_y^0 \exp(i\phi_y)] \frac{\exp[i(\omega_1 - \omega_L + \Omega)t]}{i(\omega_1 - \omega_L + \Omega)} + [E_x^0 \exp(-i\phi_x) + iE_y^0 \exp(-i\phi_y)]$$
$$\times \frac{\exp[i(\omega_1 - \omega_L - \Omega)t]}{i(\omega_1 - \omega_L - \Omega)} \Bigg) \frac{dC_1^{\dagger}(t)}{dt} + C_1^{\dagger} E_x^0 \Bigg(\exp(i\phi_x) \frac{\exp[i(\omega_1 + \Omega)t]}{i(\omega_1 + \Omega)} + \exp(-i\phi_x) \frac{\exp[i(\omega_1 - \Omega)t]}{i(\omega_1 - \Omega)} \Bigg) \frac{dC_2^{\dagger}(t)}{dt}$$
$$+ C_1^{\dagger} \Bigg([E_x^0 \exp(i\phi_x) - iE_y^0 \exp(i\phi_y)] \frac{\exp[i(\omega_1 + \omega_L + \Omega)t]}{i(\omega_1 + \omega_L + \Omega)} + [E_x^0 \exp(-i\phi_x) - iE_y^0 \exp(-i\phi_y)]$$
$$\times \frac{\exp[i(\omega_1 + \omega_L - \Omega)t]}{i(\omega_1 + \omega_L - \Omega)} \Bigg) \frac{dC_3^{\dagger}(t)}{dt} \Bigg] dt, \tag{83}$$

where $dC_1^{\dagger}(t)/dt$, $dC_2^{\dagger}(t)/dt$, and $dC_3^{\dagger}(t)/dt$ is given by replacing $C_i(t)$, $i = 1, 2, 3$ by $C_i^{\dagger}(t)$, $i = 1, 2, 3$ in Eqs. (30)–(32), respectively.

Accordingly, if

$$|C_1^0(t)|^2 \gg |V(t)|^2, \tag{84}$$

where

$$V(t) = C_1^1\left(\left[E_x^0\exp(i\phi_x) + iE_y^0\exp(i\phi_y)\right]\frac{\exp[i(\omega_1-\omega_L+\Omega)t]}{i(\omega_1-\omega_L+\Omega)} + \left[E_x^0\exp(-i\phi_x) + iE_y^0\exp(-i\phi_y)\right]\frac{\exp[i(\omega_1-\omega_L-\Omega)t]}{i(\omega_1-\omega_L-\Omega)}\right)C_4^0(t)$$
$$\times C_7^5E_x^0\left(\exp(i\phi_x)\frac{\exp[i(\omega_1+\Omega)t]}{i(\omega_1+\Omega)} + \exp(-i\phi_x)\frac{\exp[i(\omega_1-\Omega)t]}{i(\omega_1-\Omega)}\right)C_3^0(t) + C_1^1\left(\left[E_x^0\exp(i\phi_x) - iE_y^0\exp(i\phi_y)\right]\right.$$
$$\left.\times\frac{\exp[i(\omega_1+\omega_L+\Omega)t]}{i(\omega_1+\omega_L+\Omega)} + \left[E_x^0\exp(-i\phi_x) - iE_y^0\exp(-i\phi_y)\right]\frac{\exp[i(\omega_1+\omega_L-\Omega)t]}{i(\omega_1+\omega_L-\Omega)}\right)C_6^0(t) \tag{85}$$

then

$$C_1^0(t) = P_1\frac{\exp[i(\omega_0+\omega_L-\omega)t]}{i(\omega_0+\omega_L-\omega)} + V(t) - U(t), \tag{86}$$

that is, $C_1^0(t)$ is an approximate solution of Eq. (44).

From

$$|C_4^0(t)|^2, \quad |C_3^0(t)|^2, \quad |C_6^0(t)|^2 \approx \frac{Qe^2a_0^2\langle E^2\rangle}{\hbar^2\omega_1^2} \tag{87}$$

and Eq. (77), we can be sure that if

$$\frac{33(Qa_0^2)^2e^4\langle E^2\rangle}{\hbar^4\omega_1^4} \ll 1, \tag{88}$$

then Eq. (84) is valid, that is, $C_1^0(t)$ is a good approximate solution of Eq. (27). Similarly, we can prove the same for the remaining equations.

ACKNOWLEDGMENT

I thank Professor H. E. Wilhelm for technical discussions during the development of this theory.

[1]M. Baranger and B. Mozer, Phys. Rev. **123**, 25 (1961).
[2]J. Reinheimer, J. Quant. Spectrosc. Radiat. Transfer **4**, 671 (1964).
[3]W. S. Cooper and H. Ringler, Phys. Rev. **179**, 226 (1969).
[4]H.-J. Kunze, H. R. Griem, A. W. Desilva, G. C. Goldenbaum, and I. J. Spalding, Phys. Fluids **12**, 2669 (1969).
[5]W. W. Hicks, R. A. Hess, and W. S. Cooper, Phys. Rev. 5 490 (1972).
[6]D. Prosnitz, D. W. Wildman, and E. V. George, Phys. Rev. **13**, 891 (1976).
[7]S. H. Kim (unpublished).
[8]H.-J. Kunze, H. R. Griem, A. W. Desilva, G. C. Goldenbaum, and I. J. Spalding (Ref. 4) found experimentally this difference and tried to explain this intensity ratio by extending perturbation calculation up to fourth order.
[9]J. Richter, in *Plasma Diagnostics*, edited by W. Lochte-Holtgreven (North-Holland, Amsterdam, 1968) p. 28.
[10]L. I. Shiff, *Quantum Mechanics* (McGraw-Hill, New York, 1968).
[11]W. H. Louisell, *Radiation and Noise in Quantum Electronics* (McGraw-Hill, New York, 1964).
[12]E. Schrödinger, Z. Phys. **78**, 809 (1932).
[13]S. H. Kim and H. E. Wilhelm, J. Appl. Phys. **44**, 802 (1973).
[14]H. R. Griem *Special Line Broadening by Plasmas* (Academic, New York, 1974), pp. 153—162.
[15]H. R. Griem (Ref. 14) treats the spectral line shape due to the radiation field without taking into account properly the radiation field. Therefore, Griem's considerations on spectral line broadening are invalid.


ED
78